Holographic non-Gaussianities in general single-field inflation

Hiroshi Isono,[a] **Toshifumi Noumi,**[b,c] **Gary Shiu,**[b,d] **Sam S.C. Wong**[b] **and Siyi Zhou**[b]

[a]*Department of Physics, Faculty of Science,*
Chulalongkorn University, Bangkok 10330, Thailand

[b]*Department of Physics and Jockey Club Institute for Advanced Study,*
Hong Kong University of Science and Technology, Hong Kong

[c]*Department of Physics,*
Kobe University, Kobe 657-8501, Japan

[d]*Department of Physics, University of Wisconsin-Madison,*
Madison, WI 53706, U.S.A.

 E-mail: hiroshi.isono81@gmail.com, tnoumi@phys.sci.kobe-u.ac.jp,
shiu@physics.wisc.edu, scswong@ust.hk, szhouah@connect.ust.hk

ABSTRACT: We use holographic techniques to compute inflationary non-Gaussianities for general single-field inflation, including models with a non-trivial sound speed. In this holographic approach, the inflationary dynamics is captured by a relevant deformation of the dual conformal field theory (CFT) in the UV, while the inflationary correlators are computed by conformal perturbation theory. In this paper, we discuss the effects of higher derivative operators, such as $(\partial_\mu \phi \partial^\mu \phi)^m$, which are known to induce a non-trivial sound speed and source potentially large non-Gaussianities. We compute the full inflationary bispectra from the deformed CFT correlators. We also discuss the squeezed limit of the bispectra from the viewpoint of operator product expansions. As is generic in the holographic description of inflation, our power spectrum is blue tilted in the UV region. We extend our bispectrum computation to the IR region by resumming the conformal perturbations to all orders. We provide a self-consistent setup which reproduces a red tilted power spectrum, as well as all possible bispectrum shapes in the slow-roll regime.

Contents

1 Introduction

By now, there is overwhelming evidence for the celebrated AdS/CFT correspondence [1]. Given its vast successes, it is natural to wonder if there is a de Sitter counterpart. Despite the lack of an explicit string theory construction of de Sitter space, an analysis of the asymptotic symmetries along the lines of [1] suggests a similar duality between de Sitter space and conformal field theory [2, 3]. The dS/CFT correspondence states that physics in $(d+1)$ dimensional de Sitter space dS_{d+1} is dual to some conformal field theory CFT_d in d dimensional Euclidean space, of which the geometry is a constant time slice of the de Sitter spacetime. The isometry group of dS_{d+1} matches with the conformal group of Euclidean CFT_d, which is $SO(d+1,1)$. This is the starting point of the conjectured relationship between these two descriptions.

While the dS/CFT correspondence was originally introduced to discuss quantum nature of gravity on de Sitter space, it has also shed some light on observational cosmology, particularly in the context of cosmic inflation. An inflationary universe may be regarded as a quasi-de Sitter space with an approximately (but not exactly) constant Hubble parameter H. Since the time-translation invariance of de Sitter space corresponds to the scale invariance of the dual CFT, the dS/CFT correspondence has to be extended to non-conformal theories in order to capture inflationary dynamics in a holographic manner. Just as the standard AdS/CFT correspondence, it was achieved, e.g. by performing relevant deformations in the dS/CFT correspondence [4–27]. This extended relationship is sometimes dubbed the inflation/deformed CFT correspondence.

In this holographic picture the expansion history of our universe may be identified with the renormalization group (RG) flow of the field theory dual [4]. In particular the universe is asymptotically de Sitter space at the future and past infinities, corresponding to the UV and IR fixed points of the flow, with inflation in the interim (see figure 1). The slow-roll property of inflation is translated to the smallness of the beta function of the field theory dual. Based on this picture, inflationary correlation functions have been computed for some inflationary models via the relevant deformation of the field theory dual [8, 16, 19, 21, 24, 25]. It was also used to derive inflationary consistency relations based on the broken conformal symmetry [16, 27].

In light of these developments, we would like to use holographic techniques to compute inflationary non-Gaussianities for general single-field inflation [28]. Primordial non-Gaussianities, which give a direct measurement of interactions during inflation, are one of the most important probes of high energy physics in the early universe. While the level of non-Gaussianities generated by single-field inflationary models with a canonical kinetic term is suppressed by slow-roll parameters [6, 29], higher derivative interactions in the generalized Lagrangians are known to source potentially large non-Gaussianities as well as a non-trivial sound speed $c_s < 1$ [28, 30, 31]. The inflationary bispectrum for general single-field inflation has been computed directly on the inflation side long ago [28] (see [32] for a less complete result that applies only to cases with $c_s \approx 1$). It was shown that the bispectrum is completely determined by five parameters: the usual slow-roll parameters ϵ, η, the sound speed c_s and its rate of change $s := \dot{c}_s/(c_s H)$, and Λ which characterizes
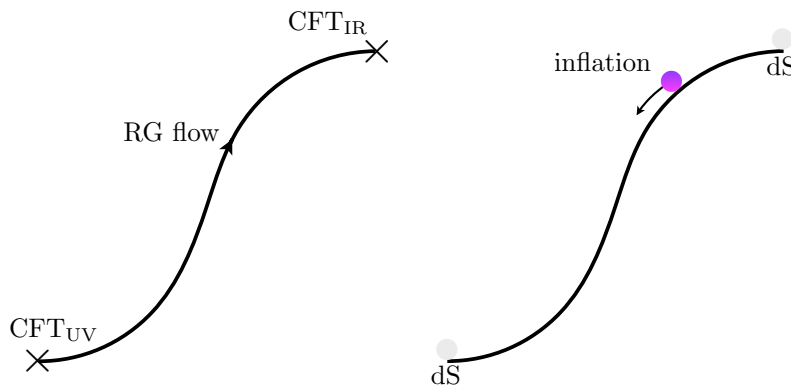
Figure 1. A sketch of the bulk and the dual CFT description of the cosmic evolution. From the bulk perspective (right figure), the inflaton starts from the grey ball on the top of the potential and rolls all the way down to the bottom of the potential. From the CFT perspective (left figure) such an evolution is identified with an RG flow connecting two conformal fixed points.

the derivative interactions [28].[1] In this paper, as a first step, we compute the bispectrum of general single-field inflation along the line of conformal perturbation theory of the CFT dual.

In order to carry out the conformal perturbation theory, we need to specify the reference CFT. However, while a concrete realization of the dS/CFT correspondence was proposed for Vasiliev's higher spin gravity [12, 20], an explicit realization for Einstein gravity is yet unknown. The holographic studies of inflation in the literature are therefore mainly classified into the following three categories:

1. Specify a concrete model of the reference CFT and the RG flow, and investigate the dual inflationary dynamics [14, 15].

2. Clarify model-independent properties of holographic inflation such as an expression of the power spectrum in terms of the beta function of the dual QFT [16, 17, 19, 24], and holographic derivation of consistency relations [16, 22, 26].

3. Specify the hypothetical reference CFT based on a concrete bulk model and the dS/CFT correspondence (sometimes called the holographic CFT in the context of AdS/CFT correspondence), and use conformal perturbation theory to compute inflationary spectra [9, 21, 23].

As we will see, the shape of the inflationary bispectrum depends on details of the CFT dual. We therefore consider that the last approach is adequate to discuss how the bispectrum shape of general single-field inflation is realized through the conformal perturbation theory. Also, it will be a useful step for further understanding of primordial non-Gaussianities from the holographic viewpoint. Based on these motivations, we employ the third approach

---

[1]Our parameter Λ was denoted by λ in [28]. We use the capital letter Λ because λ is reserved for the anomalous conformal dimension of the deformation operator O_0, which is one of the key parameters appearing recurrently in this paper. See the next section for its definition.

in the above to compute the bispectrum of general single-field inflation. In particular we reproduce the shape of the bispectrum dictated by the sound speed c_s, albeit in a perturbative manner order by order in $1 - c_s$.

The organization of the paper and main results of each section are as follows. In section 2 we review basics of holographic inflation. In particular we introduce the holographic dictionary between inflationary observables and correlators of the deformed CFT.

In section 3 we compute the inflationary bispectrum in a holographic way, using the conformal perturbation theory around the UV fixed point. We first summarize general features of holographic primordial spectra which do not depend on details of inflationary models. In particular we derive consistency relations of bispectra based on the conformal Ward identity, by extending the previous derivation at the lowest order of the conformal perturbation [16]. We then compute the bispectrum of general single-field inflation at the UV scale. Based on the third approach mentioned above, we specify the UV CFT correlators by solving the Dirichlet boundary problem of the AdS model associated with the dS dynamics of our interests. We also discuss why the bispectrum associated with higher derivative interactions vanishes in the squeezed limit, from the viewpoint of operator product expansion, which is a less model-sensitive argument based on conformal symmetry.

The inflationary spectra around the UV fixed point are known to be blue tilted. In section 4, in order to reproduce a red tilted spectrum consistent with observation [33], we extend our computation of the bispectrum to the IR region by taking into account the conformal perturbation at all orders. Under the approximation that the deformation operator is nearly marginal and the derivative interactions are reasonably small, we compute the leading contribution to the bispectrum at the IR scale and explicitly perform the resummation over the deformation parameter. We reproduce all possible bispectrum shapes of general single-field inflation in the slow-roll regime, even at the scale with the red spectrum beyond the UV scale. This is our main result in this paper. We relegate some useful details of CFT correlation functions to the appendices.

2 Holographic approach to single field inflation

In this section we summarize the basics of holographic inflation relevant to this paper [6, 16, 19, 21]. In section 2.1 we first sketch how the relevant deformation of the dual CFT can be related to the inflationary dynamics. We then in section 2.2 introduce the relation between primordial spectra and correlation functions of the field theory dual. We will apply the general results introduced here to concrete inflationary models in the following sections.

2.1 Inflation from relevant perturbations

In the holographic approach, the inflationary dynamics is captured by a relevant deformation of the dual CFT. We perturb this CFT by a relevant operator O_0 dual to the inflaton field as

$$S[\chi] = S_{\mathrm{CFT}}[\chi] + \int d^3x \, \bar{\phi} \, O_0(\boldsymbol{x}) \,, \tag{2.1}$$

where $S_{\text{CFT}}[\chi]$ is the action of the CFT, which we call the UV CFT, and χ stands for the integration variables (matter fields) of the path integral defining the UV CFT. As depicted in figure 1, the UV CFT is associated with the future infinity of an asymptotically de Sitter space. The deformation parameter $\bar{\phi}$ is related to the inflaton background value at late time corresponding to the Wilsonian cutoff scale Λ of the field theory dual as $\phi = \bar{\phi}\Lambda^{-\lambda}$. We take the limit $\Lambda \to \infty$ with $\bar{\phi}$ being fixed.

Just as the evolution of inflaton background deforms the de Sitter space and breaks some isometries, the relevant deformation O_0 breaks the conformal invariance of the dual CFT. It is instructive to see this concretely from the scale dependence of correlation functions, with an analogy to the inflationary perturbations. Correlation functions in the deformed QFT can be expressed in terms of the UV CFT correlators as

$$\langle \dots \rangle = \left\langle \dots \exp\left[-\int d^3x\, \bar{\phi}\, O_0(\boldsymbol{x})\right] \right\rangle_{\text{CFT}}, \tag{2.2}$$

where $\langle \dots \rangle_{\text{CFT}}$ is the correlation function in the UV CFT. In particular the two-point function in momentum space is given by[2]

$$\langle O_0(\boldsymbol{k})O_0(-\boldsymbol{k})\rangle' = \langle O_0(\boldsymbol{k})O_0(-\boldsymbol{k})\rangle'_{\text{CFT}} - \bar{\phi}\langle O_0(\boldsymbol{k})O_0(-\boldsymbol{k})O_0(\boldsymbol{0})\rangle'_{\text{CFT}} + \mathcal{O}(\bar{\phi}^2). \tag{2.3}$$

We have also used $\int d^3x\, O_0(\boldsymbol{x}) = O_0(\boldsymbol{k} = \boldsymbol{0})$. The scale dependence of each CFT correlator is determined by the dilatation symmetry as

$$\langle O_0(\boldsymbol{k})O_0(-\boldsymbol{k})\rangle'_{\text{CFT}} = A_0 k^{3-2\lambda}, \quad \langle O_0(\boldsymbol{k})O_0(-\boldsymbol{k})O_0(\boldsymbol{0})\rangle'_{\text{CFT}} = A_1 k^{3-3\lambda}, \tag{2.4}$$

where λ is a positive constant defined by $\lambda = 3 - \Delta$ with Δ being the scaling dimension of O_0 in the UV CFT. The coefficients A_0 and A_1 are determined only from the UV CFT data. We then have

$$\langle O_0(\boldsymbol{k})O_0(-\boldsymbol{k})\rangle' = A_0 k^{3-2\lambda}\left[1 - \frac{A_1}{A_0}\bar{\phi}k^{-\lambda} + \mathcal{O}(\bar{\phi}^2)\right]. \tag{2.5}$$

Since the deformation parameter $\bar{\phi}$ always appears with a factor $k^{-\lambda}$, the correlation functions reduce to the UV CFT ones in the limit $k \to \infty$. On the other hand, the deformation becomes important in the IR as $k \to 0$. The deformation induced momentum dependence probes the QFT at different scales, as each mode of the observed inflationary perturbations probes the geometry at its own horizon crossing time. Since holography converts the scale dependence of the QFT to the time evolution of the bulk geometry, we can compute inflationary correlation functions from the QFT correlators at an appropriate scale associated with the geometry of our interest (see figure 1). Therefore one can extract inflationary observables from QFT correlators. For instance, the spectral index $(n_s - 1)$ and its running are in principle encoded in (2.5).

---

[2]For a correlation function in momentum space we will put a prime on the bracket $\langle \dots \rangle'$, which means dropping the factor $(2\pi)^3\delta^3(\sum \boldsymbol{k}_i)$, while for a correlation function in position space we will not put a prime on the ket.

2.2 Holographic dictionary

We next introduce the holographic dictionary translating the inflationary correlation functions and the QFT correlators. For this purpose, it is convenient to start from an action with sources,

$$S[\chi; g_{ij}, \phi] = S_{\mathrm{CFT}}[\chi; g_{ij}] + \int d^3x \sqrt{g}\, \phi O_0 \,, \tag{2.6}$$

where $g_{ij}(\boldsymbol{x})$ and $\phi(\boldsymbol{x}) = \bar{\phi} + \varphi(\boldsymbol{x})$ source the energy-momentum tensor and the operator $O_0(\boldsymbol{x})$, respectively. The original action (2.1) is reproduced by setting $g_{ij} = \delta_{ij}$ and $\phi = \bar{\phi}$. The key idea of holography is that the bulk fields source operators in the dual QFT. For example, the scalar curvature perturbation ζ of inflation can be identified with the metric g_{ij} as

$$g_{ij} = e^{2\zeta}\delta_{ij} \,, \tag{2.7}$$

and sources the trace of the energy momentum tensor defined by

$$T := g^{ij} \frac{2}{\sqrt{g}} \frac{\delta S}{\delta g^{ij}} = -e^{-3\zeta} \frac{\delta S}{\delta \zeta} = -\left(\frac{\partial \mathcal{L}}{\partial \zeta} + 3\mathcal{L} \right) \,, \tag{2.8}$$

where we introduced the Lagrangian density $\mathcal{L}$ such that $S = \int d^3x \sqrt{g}\mathcal{L} = \int d^3x\, e^{3\zeta}\mathcal{L}$. Here and in what follows we drop the tensor modes and focus on the scalar sector only. For later use, it is convenient to expand the energy-momentum tensor in ζ and φ as

$$T = T_0 + T_1\zeta - 3\varphi O_0 + \dots \,, \tag{2.9}$$

where the dots stand for the second and higher orders in ζ and φ. In particular we may write T_0 and T_1 in terms of the Lagrangian density as

$$T_0 = -\left[\frac{\partial \mathcal{L}}{\partial \zeta} + 3\mathcal{L} \right]_{\substack{\zeta=0 \\ \varphi=0}} \,, \quad T_1 = -\left[\frac{\partial^2 \mathcal{L}}{\partial \zeta^2} + 3\frac{\partial \mathcal{L}}{\partial \zeta} \right]_{\substack{\zeta=0 \\ \varphi=0}} \,. \tag{2.10}$$

The action can then be expanded in ζ up to the second order as

$$S[\chi; g_{ij}, \phi] = S[\chi; \delta_{ij}, \bar{\phi}] + \int d^3x \left[\left[\frac{\partial \mathcal{L}}{\partial \zeta} + 3\mathcal{L} \right]_{\substack{\zeta=0 \\ \varphi=0}} \zeta + \frac{1}{2}\left[\frac{\partial^2 \mathcal{L}}{\partial \zeta^2} + 6\frac{\partial \mathcal{L}}{\partial \zeta} + 9\mathcal{L} \right]_{\substack{\zeta=0 \\ \varphi=0}} \zeta^2 + \dots \right]$$

$$= S[\chi; \delta_{ij}, \bar{\phi}] - \int d^3x \left[T_0\zeta + \frac{1}{2}(3T_0 + T_1)\zeta^2 + \dots \right] \,, \tag{2.11}$$

where note that the dots contain terms with φ as well as higher order terms in ζ. In the following we mostly use $U = 3T_0 + T_1$ instead of T_1 for notational simplicity.

The holographic dictionary relates the bulk wave function $\Psi[\zeta]$ and the QFT partition function $Z[\zeta]$ as [6]

$$\Psi[\zeta] = Z[\zeta] \,. \tag{2.12}$$

Here $\Psi[\zeta]$ is the wavefunction of ζ at the future infinity in the gauge $\phi(\boldsymbol{x},t) = \bar{\phi}(t)$.[3] On the other hand, we define the partition function in the dual QFT by

$$Z[\zeta] := \int [d\chi] e^{-S[\chi; g_{ij}, \bar{\phi}]} \quad \text{with} \quad g_{ij} = e^{2\zeta} \delta_{ij}. \tag{2.13}$$

We normalize it so that $Z[\zeta = 0] = 1$. It can then be expanded in ζ as

$$\begin{aligned}
Z[\zeta] = \exp\bigg[&\frac{1}{2} \int d^3 x_1 d^3 x_2 \langle T_0(\boldsymbol{x}_1) T_0(\boldsymbol{x}_2)\rangle \zeta(\boldsymbol{x}_1) \zeta(\boldsymbol{x}_2) \\
&+ \frac{1}{6} \int d^3 x_1 d^3 x_2 d^3 x_3 \big[\langle T_0(\boldsymbol{x}_1) T_0(\boldsymbol{x}_2) T_0(\boldsymbol{x}_3)\rangle \\
&+ 3 \langle T_0(\boldsymbol{x}_1) U(\boldsymbol{x}_2)\rangle \delta^3(\boldsymbol{x}_2 - \boldsymbol{x}_3) \big] \zeta(\boldsymbol{x}_1) \zeta(\boldsymbol{x}_2) \zeta(\boldsymbol{x}_3) + \mathcal{O}(\zeta^4) \bigg]. \tag{2.14}
\end{aligned}$$

Here and in what follows we drop ultra-local terms, which contain two or more delta functions and are not important for our purpose. We also assume that one-point functions vanish.[4] The correlation functions $\langle \dots \rangle$ on the right hand side are defined with the action $S[\chi; \delta_{ij}, \bar{\phi}]$. By going into the momentum space and identifying $Z[\zeta]$ with the wave function $\Psi[\zeta]$, we can write primordial spectra in terms of correlation functions in the dual QFT as

$$\langle \zeta(\boldsymbol{k}) \zeta(-\boldsymbol{k})\rangle' = \frac{1}{-2\mathrm{Re}\langle T_0(\boldsymbol{k}) T_0(-\boldsymbol{k})\rangle'}, \tag{2.15}$$

$$\langle \zeta(\boldsymbol{k}_1) \zeta(\boldsymbol{k}_2) \zeta(\boldsymbol{k}_3)\rangle' = \frac{2\mathrm{Re}\langle T_0(\boldsymbol{k}_1) T_0(\boldsymbol{k}_2) T_0(\boldsymbol{k}_3)\rangle' + 2\mathrm{Re}\langle T_0(\boldsymbol{k}_1) U(-\boldsymbol{k}_1)\rangle' + 2\,\mathrm{perms}}{\prod_{i=1}^3 \left[-2\mathrm{Re}\langle T_0(\boldsymbol{k}_i) T_0(-\boldsymbol{k}_i)\rangle' \right]}, \tag{2.16}$$

where the correlators of ζ on the left hand side are defined by $\langle \dots \rangle = \int [d\zeta] \dots |\Psi[\zeta]|^2$.

Finally, we reformulate the dictionary (2.15)–(2.16) in terms of correlation functions of O_0 by using the conformal Ward-Takahashi identity [34, 35]

$$\langle T(\boldsymbol{x})\rangle_s = -\lambda \phi(\boldsymbol{x}) \langle O_0(\boldsymbol{x})\rangle_s = -\lambda \left(\bar{\phi} + \varphi(\boldsymbol{x}) \right) \langle O_0(\boldsymbol{x})\rangle_s, \tag{2.17}$$

where $\langle \dots \rangle_s$ is the correlation function computed in the presence of the sources ζ and φ. Expanding this master equation in ζ and φ, we can convert the T_0 correlators into O_0 correlators. For example, the order ζ^1 and φ^1 terms of eq. (2.17) are given by

$$\langle T_0(\boldsymbol{k}) T_0(-\boldsymbol{k})\rangle' + \langle T_1(\boldsymbol{0})\rangle' = -\lambda \bar{\phi} \langle T_0(\boldsymbol{k}) O_0(-\boldsymbol{k})\rangle', \tag{2.18}$$

$$\langle T_0(\boldsymbol{k}) O_0(-\boldsymbol{k})\rangle' + 3 \langle O_0(\boldsymbol{0})\rangle' = -\lambda \bar{\phi} \langle O_0(\boldsymbol{k}) O_0(-\boldsymbol{k})\rangle' + \lambda \langle O_0(\boldsymbol{0})\rangle', \tag{2.19}$$

where we used the expression (2.9). We then arrive at the relation,

$$\begin{aligned}
\langle T_0(\boldsymbol{k}) T_0(-\boldsymbol{k})\rangle' &= \lambda^2 \bar{\phi}^2 \langle O_0(\boldsymbol{k}) O_0(-\boldsymbol{k})\rangle' + (3-\lambda)\lambda \bar{\phi} \langle O_0(\boldsymbol{0})\rangle' - \langle T_1(\boldsymbol{0})\rangle' \\
&= \lambda^2 \bar{\phi}^2 \langle O_0(\boldsymbol{k}) O_0(-\boldsymbol{k})\rangle', \tag{2.20}
\end{aligned}$$

---

[3]See, e.g., [18, 19, 23, 27] for other gauge choices.

[4]If one takes into account the quadratic order $\frac{1}{2} T_2 \zeta^2$ in T in eq. (2.9), it contributes to a contact term in the coefficient of $\zeta(\boldsymbol{x})^3$, where all operators overlap at the same point $\boldsymbol{x}$. In principle, these contact terms are canceled by local counterterms.

where at the second equality we assumed that one-point functions of O_0 and T_1 vanish. Similarly we can derive the relation,

$$\langle T_0(\boldsymbol{k}_1)T_0(\boldsymbol{k}_2)T_0(\boldsymbol{k}_3)\rangle' + \langle U(\boldsymbol{k}_1)T_0(-\boldsymbol{k}_1)\rangle' + \langle U(\boldsymbol{k}_2)T_0(-\boldsymbol{k}_2)\rangle' + \langle U(\boldsymbol{k}_3)T_0(-\boldsymbol{k}_3)\rangle'$$
$$= -\lambda^3\bar{\phi}^3\langle O_0(\boldsymbol{k}_1)O_0(\boldsymbol{k}_2)O_0(\boldsymbol{k}_3)\rangle'$$
$$+ \lambda^3\bar{\phi}^2\Big[\langle O_0(\boldsymbol{k}_1)O_0(-\boldsymbol{k}_1)\rangle' + \langle O_0(\boldsymbol{k}_2)O_0(-\boldsymbol{k}_2)\rangle' + \langle O_0(\boldsymbol{k}_3)O_0(-\boldsymbol{k}_3)\rangle'\Big]. \quad (2.21)$$

We therefore have

$$\langle \zeta(\boldsymbol{k})\zeta(-\boldsymbol{k})\rangle' = \frac{1}{\lambda^2\bar{\phi}^2\left[-2\mathrm{Re}\langle O_0(\boldsymbol{k})O_0(-\boldsymbol{k})\rangle'\right]}, \quad (2.22)$$

$$\langle \zeta(\boldsymbol{k}_1)\zeta(\boldsymbol{k}_2)\zeta(\boldsymbol{k}_3)\rangle' = \frac{-2\bar{\phi}\mathrm{Re}\langle O_0(\boldsymbol{k}_1)O_0(\boldsymbol{k}_2)O_0(\boldsymbol{k}_3)\rangle' + 2\mathrm{Re}\langle O_0(\boldsymbol{k}_1)O_0(-\boldsymbol{k}_1)\rangle' + 2\,\mathrm{perms}}{\lambda^3\bar{\phi}^4\prod_{i=1}^3\left[-2\mathrm{Re}\langle O_0(\boldsymbol{k}_i)O_0(-\boldsymbol{k}_i)\rangle'\right]}.$$
$$(2.23)$$

Interestingly, no correlation functions including U appear in these relations. As a result we can compute primordial spectra purely in terms of correlation functions of O_0 together with the parameters λ and $\bar{\phi}$.

3 The UV story

In this section we compute the inflationary bispectrum in a class of $P(X,\phi)$ inflation models by using the perturbed CFT presented in the last section. As we discussed in the last section, the perturbation from the UV CFT corresponds to the perturbative expansion in $\bar{\phi}k^{-\lambda}$. In this section we focus on the UV region, where higher order terms in $\bar{\phi}k^{-\lambda}$ are negligible. In the next section we extend our result to the IR region by performing a resummation.

3.1 Generality and consistency relation of bispectrum

Let us first discuss general properties of holographic inflationary correlation functions. As we mentioned earlier, correlation functions in the dual QFT are expanded in the deformation parameter $\bar{\phi}$. Each order of a two-point function in $\bar{\phi}$ is determined by the dilatation symmetry up to a constant as

$$\langle O_0(\boldsymbol{k})O_0(-\boldsymbol{k})\rangle' = k^{3-2\lambda}\sum_{n=0}^{\infty} A_n\left(-\bar{\phi}k^{-\lambda}\right)^n. \quad (3.1)$$

where A_0 and A_1 are given by (2.4) and other A_n's are defined in a similar way. They are uniquely determined by the UV CFT data, i.e., the spectrum and the OPE coefficients of the UV CFT. Note also that A_n's are real constants because O_0 is a real scalar. Through the holographic dictionary (2.22), the inflationary power spectrum is given by

$$\mathcal{P}_\zeta(k) = \frac{k^3}{2\pi^2}\langle \zeta(\boldsymbol{k})\zeta(-\boldsymbol{k})\rangle' = \frac{k^{2\lambda}}{2\pi^2(-2\lambda^2\bar{\phi}^2)}\left[\sum_{n=0}^{\infty} A_n\left(-\bar{\phi}k^{-\lambda}\right)^n\right]^{-1}. \quad (3.2)$$

We may compute the corresponding spectral index as

$$n_s - 1 = \frac{d \ln \mathcal{P}_\zeta}{d \ln k} = 2\lambda + \lambda \frac{\sum n A_n \left(-\bar{\phi} k^{-\lambda}\right)^n}{\sum A_n \left(-\bar{\phi} k^{-\lambda}\right)^n}$$
$$= \lambda \left[2 + \frac{A_1}{A_0}(-\bar{\phi} k^{-\lambda}) + \left(2\frac{A_2}{A_0} - \frac{A_1^2}{A_0^2}\right)\left(-\bar{\phi} k^{-\lambda}\right)^2 + \ldots \right]. \quad (3.3)$$

Notice that the spectrum is blue tilted, i.e., $n_s - 1 > 0$, in the UV region because the UV CFT is deformed by a relevant operator $\lambda > 0$. Therefore we need to go to the IR region to reproduce a red spectrum.

In the inflationary context it is common to normalize the bispectrum by a factor of the power spectrum squared. By using the dictionary (2.22) and (2.23), we may express the normalized bispectrum in terms of the O_0 correlators as

$$\frac{\langle \zeta(\boldsymbol{k}_1)\zeta(\boldsymbol{k}_2)\zeta(\boldsymbol{k}_3)\rangle'}{\langle \zeta(\boldsymbol{k}_1)\zeta(-\boldsymbol{k}_1)\rangle'\langle \zeta(\boldsymbol{k}_2)\zeta(-\boldsymbol{k}_2)\rangle'} = -\lambda \left(1 + \frac{\mathrm{Re}\langle O_0(\boldsymbol{k}_2)O_0(-\boldsymbol{k}_2)\rangle'}{\mathrm{Re}\langle O_0(\boldsymbol{k}_3)O_0(-\boldsymbol{k}_3)\rangle'} + \frac{\mathrm{Re}\langle O_0(\boldsymbol{k}_1)O_0(-\boldsymbol{k}_1)\rangle'}{\mathrm{Re}\langle O_0(\boldsymbol{k}_3)O_0(-\boldsymbol{k}_3)\rangle'}\right)$$
$$+ \lambda\bar{\phi}\frac{\mathrm{Re}\langle O_0(\boldsymbol{k}_1)O_0(\boldsymbol{k}_2)O_0(\boldsymbol{k}_3)\rangle'}{\mathrm{Re}\langle O_0(\boldsymbol{k}_3)O_0(-\boldsymbol{k}_3)\rangle'}. \quad (3.4)$$

By a similar argument for the power spectrum case, we may rewrite it in terms of the UV CFT correlators. Later we will do that explicitly for a concrete UV CFT, but in the rest of this subsection we focus on the squeezed limit without specifying the detail of the UV CFT. In the squeezed limit $k_1 \ll k_2 = k_3$, the normalized bispectrum (3.4) is reduced to the form,

$$\frac{\langle \zeta(\boldsymbol{k}_1)\zeta(\boldsymbol{k}_2)\zeta(\boldsymbol{k}_3)\rangle'}{\langle \zeta(\boldsymbol{k}_1)\zeta(-\boldsymbol{k}_1)\rangle'\langle \zeta(\boldsymbol{k}_2)\zeta(-\boldsymbol{k}_2)\rangle'} \to -2\lambda + \lambda\bar{\phi}\frac{\mathrm{Re}\langle O_0(\boldsymbol{0})O_0(\boldsymbol{k}_2)O_0(-\boldsymbol{k}_2)\rangle'}{\mathrm{Re}\langle O_0(\boldsymbol{k}_2)O_0(-\boldsymbol{k}_2)\rangle'}. \quad (3.5)$$

In the inflationary context, the consistency relation, i.e., the Ward-Takahashi identity for the broken de Sitter symmetry, tells us that the shape function in the squeezed limit is related to the spectral index n_s as [6, 36]

$$\frac{\langle \zeta(\boldsymbol{k}_1)\zeta(\boldsymbol{k}_2)\zeta(\boldsymbol{k}_3)\rangle'}{\langle \zeta(\boldsymbol{k}_1)\zeta(-\boldsymbol{k}_1)\rangle'\langle \zeta(\boldsymbol{k}_2)\zeta(-\boldsymbol{k}_2)\rangle'} \to -(n_s - 1), \quad (3.6)$$

where the spectral index is computed at the horizon crossing time of the modes $\boldsymbol{k}_2 = -\boldsymbol{k}_3$.

Let us reproduce this relation from the QFT side using the expression (3.5). Since the operator $O_0(\boldsymbol{0})$ with zero momentum is sourced by the deformation parameter $\bar{\phi}$, as is seen from the deformed action (2.1), we may rewrite the second term of (3.5) as

$$\lambda\bar{\phi}\frac{\mathrm{Re}\langle O_0(\boldsymbol{0})O_0(\boldsymbol{k}_2)O_0(-\boldsymbol{k}_2)\rangle'}{\mathrm{Re}\langle O_0(\boldsymbol{k}_2)O_0(-\boldsymbol{k}_2)\rangle'} = -\lambda\bar{\phi}\frac{\partial_{\bar{\phi}}\mathrm{Re}\langle O_0(\boldsymbol{k}_2)O_0(-\boldsymbol{k}_2)\rangle'}{\mathrm{Re}\langle O_0(\boldsymbol{k}_2)O_0(-\boldsymbol{k}_2)\rangle'} = -\lambda\frac{\sum n A_n \left(-\bar{\phi} k_2^{-\lambda}\right)^n}{\sum A_n \left(-\bar{\phi} k_2^{-\lambda}\right)^n}. \quad (3.7)$$

By comparing this with the spectral index in eq. (3.3) (after the replacement $k \to k_2$), we can readily find that the consistency relation (3.6) holds for any inflationary three-point
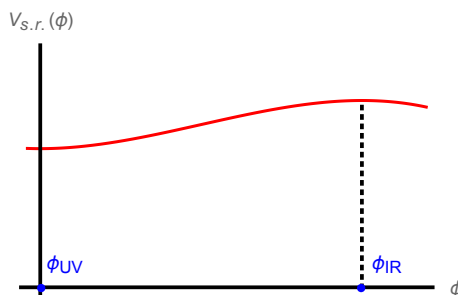
Figure 2. Illustration of the slow-roll potential $V_{\text{s.r.}}(\phi)$.

function computed via holography for any single-field inflation.[5] It should be noticed that the dilatation symmetry of the UV CFT plays a crucial role in our derivation. As mentioned in the last section, the deformation parameter $\bar{\phi}$ appears in the two-point function always in the form $\bar{\phi}k^{-\lambda}$ as a consequence of the dilatation symmetry. As a result, we may convert a derivative in $\bar{\phi}$ into that in the momentum k,

$$-\lambda \frac{\partial}{\partial \ln \bar{\phi}} \ln \left[\sum_{n=1}^{\infty} A_n \left(-\bar{\phi}k^{-\lambda} \right)^n \right] = \frac{\partial}{\partial \ln k} \ln \left[\sum_{n=1}^{\infty} A_n \left(-\bar{\phi}k^{-\lambda} \right)^n \right], \qquad (3.8)$$

to reproduce the consistency relation.

3.2 Inflationary setup

In the last subsection we showed that the three-point function in the squeezed limit is governed by the (broken) dilatation symmetry and its behavior does not depend on the details of the model. In contrast, the shape of three-point functions for general momentum configurations highly depends on the inflationary model. In the rest of this paper we specify a concrete UV CFT model and compute the shape function through the dictionary (2.23) and the conformal perturbation theory.

As we mentioned in Introduction, we would like to take into account higher derivative operators of general single-field inflation in the holographic inflation. To clarify our setup, let us begin by briefly reviewing the slow-roll inflationary models discussed in the holographic context:

$$S_{\text{s.r.}} = \int d^4x \sqrt{-g} \left[\frac{M_{\text{Pl}}^2}{2} R - \frac{1}{2}(\partial_\mu \phi)^2 - V_{\text{s.r.}}(\phi) \right]$$

with $\qquad V_{\text{s.r.}}(\phi) = 3M_{\text{Pl}}^2 H_0^2 + \frac{m^2}{2}\phi^2 - \frac{g_3}{3}\phi^3 + \mathcal{O}(\phi^4).$ $\qquad (3.9)$

Here the inflaton mass m and the scaling dimension $\Delta = 3 - \lambda$ of the operator O_0 dual to the inflaton are related by $m^2 = \lambda(3 - \lambda)H_0^2$. We assume that $\lambda \ll 1$ for the slow-roll property. We also assume that $g_3 \sim 1$ to make the conformal perturbation work well

---

[5]A similar derivation is given in [16] at the leading order in $\bar{\phi}$. Our derivation can be thought of as its all-order extension. Another type of holographic derivation may be found in [26, 39], where an infinite set of consistency relations [38] were derived (at all orders in $\bar{\phi}$) based on diffeomorphism invariance of the field theory dual or equivalently spatial diffeomorphism invariance on the constant time slice.

throughout the RG flow generated by the deformation of the CFT.[6] As depicted in figure 2, this potential has two extrema,

$$\phi_{\text{UV}} = 0\,, \quad \phi_{\text{IR}} = \frac{3\lambda H_0^2}{g_3} + \mathcal{O}(\lambda^2)\,, \tag{3.10}$$

which correspond to the dual UV and IR CFTs, respectively. We may find a time-dependent solution connecting the two extrema,

$$\phi(t) = \phi_* \frac{1}{e^{\lambda H_0(t-t_*)} + (1 - e^{\lambda H_0(t-t_*)})\frac{g_3\phi_*}{3\lambda H_0^2}}\,, \tag{3.11}$$

which satisfies the Hamilton-Jacobi equation for a spatially homogeneous configuration,

$$\dot{\phi} \simeq -\lambda H_0\phi + \frac{g_3}{3H_0}\phi^2\,, \tag{3.12}$$

in the regime $\lambda \ll 1$. Here we introduced $\phi(t_*) = \phi_*$ with t_* being some reference time. The inflaton background evolution (3.11) can then be identified with the RG flow connecting the two CFTs. Also let us recall that the scalar spectral index is directly related to the scaling dimension of the deformation operator [see, e.g., eq. (3.3)]. Since the deformation operator is relevant (irrelevant) near the UV (IR) fixed point, the scalar power spectrum is blue (red) tilted in the UV (IR) region [17, 21, 24].

Let us now add higher derivative operators to the above slow-roll model. The general single-field inflation, or the so-called $P(X, \phi)$ model, has an action of the form,

$$S = \int d^4x\sqrt{-g}\left[\frac{M_{\text{Pl}}^2}{2}R + P(X, \phi)\right]\,, \tag{3.13}$$

where $P(X, \phi)$ is an arbitrary function of the inflaton ϕ and its kinetic operator $X = -\frac{1}{2}(\partial_\mu\phi)^2$. To discuss the bispectrum associated with higher derivative operators in general single-field inflation, it will be reasonable to focus on the following class of $P(X, \phi)$ model:[7]

$$P(X, \phi) = X + \sum_{m\geq 2}\alpha_m X^m - V_{\text{s.r.}}(\phi)\,, \tag{3.14}$$

where $V_{\text{s.r.}}(\phi)$ is the slow-roll potential in eq. (3.9). Although our model (3.14) accommodates stationary classical solutions $\phi = 0$ and $\phi = \phi_{\text{IR}}$, it does not necessarily mean that there exists a classical solution connecting the two extrema (corresponding to the RG flow connecting the two CFTs). Indeed, there is no such flow when α_m's are big, essentially because the slow-roll potential makes a subdominant contribution to the inflaton dynamics. In order to discuss a self-contained model with both the red tilted power spectrum and the non-Gaussianities in general single-field inflation, we focus on the following parameter region in this paper: for each $m \geq 2$

$$\lambda \ll \alpha_m\lambda^{4(m-1)} \ll 1\,. \tag{3.15}$$

---

[6]More precisely, we assume that the mass term and the cubic interaction dominate over the other terms throughout the flow.

[7]In other words, we assume $P_{X\phi} = 0$ (for any ϕ and X) for simplicity. Here and in what follows we use the notation such as $P_{X\phi} = \partial^2 P/\partial X\partial\phi$.

As we discuss in section 4, there exists an RG flow connecting the two CFTs in this parameter region. Also the sound speed c_s of the scalar perturbation satisfies $\lambda \ll c_s^{-2} - 1 \lesssim 1$ in the IR region. As a result, the bispectrum associated with the non-trivial sound speed dominates over the slow-roll type one. This is the inflationary setup we consider in this paper. It should be noted that if we are not interested in reproducing a red tilted power spectrum, we do not have to introduce the slow-roll potential. We may also relax the condition (3.15) to realize a small sound speed $c_s \ll 1$ and a large non-Gaussianity $f_{\mathrm{NL}} \gg 1$ even in the UV region. However, we focus on our parameter set to reproduce the red tilted spectrum in this paper.

3.3 UV CFT

We then would like to specify the UV CFT corresponding to the local minimum $\phi = 0$ to apply the conformal perturbation theory. As we mentioned in Introduction, we use the dS/CFT correspondence to specify the hypothetical UV CFT in this paper.

As explained in [6], the dS/CFT correspondence can be related to the AdS/CFT correspondence by an analytic continuation. If we write the Poincaré metrics of dS and Euclidean AdS as

$$ds^2_{\mathrm{dS}} = R^2_{\mathrm{dS}} \eta^{-2}(-d\eta^2 + d\boldsymbol{x}^2), \quad ds^2_{\mathrm{AdS}} = R^2_{\mathrm{AdS}} z^{-2}(dz^2 + d\boldsymbol{x}^2), \tag{3.16}$$

they are related to each other by the analytic continuation[8]

$$z = -i\eta, \quad R_{\mathrm{AdS}} = -iR_{\mathrm{dS}}, \tag{3.17}$$

where R_{dS} and R_{AdS} are the dS radius and the AdS radius, respectively. In particular, the dS radius is the inverse of the Hubble parameter H_0.[9] Furthermore, we can show that the analytic continuation (3.17) relates the perturbation theory around $\phi = 0$ (corresponding to an exact dS background) to the AdS perturbation theory of the following action:

$$S_{\mathrm{AdS}} = \int d^4x \sqrt{G}\left[\frac{1}{2}(\partial\Phi)^2 + V(\Phi) + \sum_{m \geq 2}\frac{a_m}{2^m}(\partial\Phi)^{2m}\right] \tag{3.18}$$

with the potential $V(\Phi)$ and the coupling a_m of the form,

$$V(\Phi) = \frac{m^2}{2}\Phi^2 - \frac{g_3}{3}\Phi^3 + \mathcal{O}(\Phi^4), \quad a_m = (-1)^{m+1}\alpha_m. \tag{3.19}$$

Here for simplicity we neglected gravitational fluctuations, which are not relevant to our computation. We also introduced G and Φ to denote the AdS metric and the scalar field, respectively, to avoid notational confusion. Just as the original argument in [6], our UV

---

[8]The dS/CFT correspondence and AdS/CFT correspondence can also be related by an analytic continuation of the Planck mass [10, 11]. The relation of these two approaches was discussed, e.g., in [25].

[9]The Hubble parameter of the exact dS (dual to the UV CFT) is given by H_0 introduced in eq. (3.9), whereas the Hubble parameter $H(t)$ during inflation is time-dependent and deviates from H_0 because of the inflaton background.
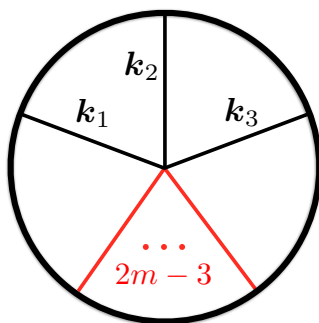
Figure 3. The Witten diagram for $\langle O_0(\boldsymbol{k}_1)O_0(\boldsymbol{k}_2)O_0(\boldsymbol{k}_3)O_0^{2m-3}(\boldsymbol{0})\rangle'_{\mathrm{CFT}}$. The black line denotes the bulk-boundary propagator $\mathcal{K}_{\boldsymbol{k}_i}(z)$. The red line represents the zero-momentum bulk-boundary propagator $\mathcal{K}_{\boldsymbol{0}}(z)$.

CFT correlation functions are then computed via the Witten diagrams for this AdS model followed by the replacement

$$R_{\mathrm{AdS}} = -iR_{\mathrm{dS}}, \quad a_m = (-)^{m+1}\alpha_m\,. \tag{3.20}$$

In the following we will compute the hypothetical UV CFT correlation functions based on this approach. Since the calculation is a bit complicated essentially because of the singularity in the limit $\lambda \to 0$, we put the details in appendices A and B, and summarize the results and the essence of our computation in the main text. Also for simplicity we mostly set $R_{\mathrm{dS}} = 1$ in the following.

3.4 Bispectrum at the UV

We then compute the three-point function of O_0 using the conformal perturbation theory for the model (3.14). As we mentioned earlier, in this section we focus on the UV region defined by

$$\bar{\phi}k^{-\lambda} \ll \lambda\,, \tag{3.21}$$

where k is a typical momentum scale of correlation functions of our interest. In this UV region, there are two types of the leading contributions to the three-point functions (3.4). The first contribution is from the first term of (3.4) and is the zeroth order in $\bar{\phi}$:

$$-\lambda \left[1 + \left(\frac{k_2}{k_3}\right)^{3-2\lambda} + \left(\frac{k_1}{k_3}\right)^{3-2\lambda}\right]\,, \tag{3.22}$$

which corresponds to the slow-roll type shape associated with the η parameter [6].

The other contribution is the α_m^1-terms of the second term of (3.4), which corresponds to the Witten diagram in figure 3. In this paper, we are interested in the leading order in λ according to the parameter regime (3.15). Noting that the integral for this Witten diagram is not singular as $\lambda \to 0$,[10] we can easily evaluate the integral at the leading order

---

[10]See also the comment at the end of section 4.1.3.

in λ. The result is

$$\lambda\bar{\phi}\frac{\text{Re}\langle O_0(\boldsymbol{k}_1)O_0(\boldsymbol{k}_2)O_0(\boldsymbol{k}_3)\rangle'}{\text{Re}\langle O_0(\boldsymbol{k}_3)O_0(-\boldsymbol{k}_3)\rangle'} \ni \frac{4k_1k_2k_3}{k_2^3}\mathcal{F}\left(\frac{k_1}{k_3},\frac{k_2}{k_3}\right), \qquad (3.23)$$

where the shape function $\mathcal{F}$ is defined as

$$\mathcal{F}\left(\frac{k_1}{k_3},\frac{k_2}{k_3}\right) = \left[-\frac{4}{3}X^2 P_{XXX}\frac{3k_1k_2k_3}{2(k_1+k_2+k_3)^3} + 2XP_{XX}G(k_1,k_2,k_3)\right]_{X=(-\lambda\bar{\phi})^2/2}. \qquad (3.24)$$

Here we introduced $P_{XX} = \partial^2 P/\partial X^2$ and $P_{XXX} = \partial^3 P/\partial X^3$. The function G is defined as

$$\begin{aligned}
G(k_1,k_2,k_3) = &-\frac{k_1^2k_2^2 + k_1^2k_3^2 + k_2^2k_3^2}{k_1k_2k_3(k_1+k_2+k_3)} \\
&+ \frac{k_1^2k_2^3 + k_1^2k_3^3 + k_2^2k_3^3 + k_2^2k_1^3 + k_3^2k_1^3 + k_3^2k_2^3}{2k_1k_2k_3(k_1+k_2+k_3)^2} + \frac{k_1^3+k_2^3+k_3^3}{8k_1k_2k_3}.
\end{aligned} \qquad (3.25)$$

This result reproduces the shapes associated with the X^m coupling computed in [28]. We may observe that the first contribution (3.22) is responsible for the consistency relation, whereas the second contribution (3.23) vanishes in the squeezed limit. Indeed, the inflationary parameters in the UV region are given by[11]

$$\epsilon = \frac{1}{2}\left(\lambda\bar{\phi}k^{-\lambda}\right)^2, \qquad (3.26)$$

$$\eta = -2\lambda, \qquad (3.27)$$

$$\frac{1}{c_s^2} - 1 = \sum_{m\geq 2}\frac{m(m-1)}{2^{m-2}}\alpha_m\left(\lambda\bar{\phi}k^{-\lambda}\right)^{2m-2}, \qquad (3.28)$$

$$s := \frac{\dot{c}_s}{Hc_s} = \sum_{m\geq 2}\frac{m(m-1)^2}{2^{m-2}}\lambda\,\alpha_m(\bar{\lambda}\phi k^{-\lambda})^{2m-2}. \qquad (3.29)$$

We may easily check that our three-point functions are consistent with the inflationary results in [28].

In the rest of this section, we revisit the shape of bispectrum associated with the higher derivative operators, i.e., the $\mathcal{O}(\alpha_m)$ contribution (3.23) from the OPE perspective. In particular we discuss why it vanishes in the squeezed limit. Let us consider the CFT correlation functions of the form,

$$\langle O_0(\boldsymbol{k}_1)O_0(\boldsymbol{k}_2)O_0(\boldsymbol{k}_3)O_0(\boldsymbol{0})\ldots O_0(\boldsymbol{0})\rangle'_{\text{CFT}}. \qquad (3.30)$$

As we have discussed, such correlation functions constitute three-point functions of the deformed CFT. In particular, they are relevant to the $\mathcal{O}(\alpha_m)$ contribution to the bispectrum. In the momentum space, the conformal partial wave expansion simply reads

$$\begin{aligned}
&\langle O_0(\boldsymbol{k}_1)O_0(\boldsymbol{k}_2)O_0(\boldsymbol{k}_3)O_0(\boldsymbol{0})\ldots O_0(\boldsymbol{0})\rangle'_{\text{CFT}} \\
&= \sum_I \frac{\langle O_0(\boldsymbol{k}_1)O_0(\boldsymbol{k}_2)O_I(\boldsymbol{k}_3)\rangle'_{\text{CFT}}\langle O_I(\boldsymbol{k}_3)O_0(-\boldsymbol{k}_3)O_0(\boldsymbol{0})\ldots O_0(\boldsymbol{0})\rangle'_{\text{CFT}}}{\langle O_I(\boldsymbol{k}_3)O_I(-\boldsymbol{k}_3)\rangle'_{\text{CFT}}}, \quad (3.31)
\end{aligned}$$

---

[11]Our convention for the slow-roll parameters is $\epsilon = -\dot{H}/H^2$ and $\eta = \dot{\epsilon}/(\epsilon H)$, where $H(t)$ is the Hubble parameter.

where O_I's denote all the primary operators in the CFT. The shape of each term in the summation is determined by the three-point functions, $\langle O_0(\boldsymbol{k}_1)O_0(\boldsymbol{k}_2)O_I(\boldsymbol{k}_3)\rangle'_{\text{CFT}}$, which is uniquely fixed by the conformal symmetry up to an overall OPE coefficient. For example, when O_I is a primary scalar, it takes the form,

$$\langle O_0(\boldsymbol{k}_1)O_0(\boldsymbol{k}_2)O_I(\boldsymbol{k}_3)\rangle'_{\text{CFT}}$$

$$= C_{O_0 O_0 O_I} k_1^{\frac{3}{2}-\lambda} k_2^{\frac{3}{2}-\lambda} k_3^{\Delta_I - \frac{3}{2}} \int_0^\infty dx\, x^{\frac{1}{2}} K_{\frac{3}{2}-\lambda}(k_1 x) K_{\frac{3}{2}-\lambda}(k_2 x) K_{\Delta_I - \frac{3}{2}}(k_3 x)\,, \quad (3.32)$$

where Δ_I is the conformal dimension of O_I. In appendix C, we compute CFT three-point functions with two nearly marginal primary scalars and one primary scalar with a conformal dimension close to a non-negative integer n. There we find that such three-point functions vanish in the squeezed limit $k_1 \ll k_2 = k_3$ except for the case $n = 0, 3$. In particular the bispectrum associated with derivative couplings is independent of the inflaton cubic coupling g_3, so that it will be dominated by the partial wave where O_I is composite (multi-trace), e.g., operators schematically of the form $O_0 \partial^p O_0$ ($p = 0, 1, 2, \ldots$). Since O_0 is nearly marginal, such composite operators have nearly integer dimensions with $n \geq 6$, and therefore their partial wave contributions vanish in the squeezed limit. The bispectrum associated with the higher derivative operators X^m then vanishes in the squeezed limit as long as this feature survives after summing up all the partial waves. Further progress in obtaining the precise momentum dependence would require a clarification of the OPE coefficients, which we postpone for future work.

4 Beyond the UV

As described in Introduction, the bulk geometry of our setup is asymptotically de Sitter space both at the early and late time. In the dual QFT point of view, we have an RG flow between an IR CFT and a UV CFT. In [17, 21] it was found that the potential (3.9) has two local extremal points corresponding to those two CFTs, each of which reproduces the spectral tilt,

$$(n_s - 1)|_{\text{UV}} = 2\lambda, \quad (n_s - 1)|_{\text{IR}} = -2\lambda + \ldots\,. \quad (4.1)$$

In this section, to discuss inflationary models with a red tilted spectrum (consistent with observations [33]), we extend the holographic computation of the bispectrum to the IR region characterized by $\bar{\phi} k^{-\lambda} \gtrsim \lambda$, in contrast with (3.21).

4.1 Inflationary bispectrum at the IR

For the holographic computation of the bispectrum (3.4), we need the two-point function

$$\langle O_0(\boldsymbol{k}_1)O_0(\boldsymbol{k}_2)\rangle' = \sum_{n=0}^\infty \frac{(-\bar{\phi})^n}{n!} \langle O_0(\boldsymbol{k}_1)O_0(\boldsymbol{k}_2)O_0(\boldsymbol{0})^n\rangle'_{\text{CFT}}\,, \quad (4.2)$$

and the three-point function

$$\langle O_0(\boldsymbol{k}_1)O_0(\boldsymbol{k}_2)O_0(\boldsymbol{k}_3)\rangle' = \sum_{n=0}^\infty \frac{(-\bar{\phi})^n}{n!} \langle O_0(\boldsymbol{k}_1)O_0(\boldsymbol{k}_2)O_0(\boldsymbol{k}_3)O_0(\boldsymbol{0})^n\rangle'_{\text{CFT}}\,, \quad (4.3)$$

– 15 –

in the deformed CFT. Just as we did in the previous section, we will compute these UV CFT correlation functions via the Witten diagrams in AdS$_4$ followed by the replacement (3.20). In the IR region, higher-point CFT correlators become non-negligible, so it seems impossible to obtain the full correlators of the deformed CFT. Nevertheless, it turns out that the leading contributions in our parameter regime are calculable by performing a resummation over $\bar{\phi}k^{-\lambda}$. For concreteness (and as it turns out to be the most relevant for our purpose), we first summarize our main results of the resummation for the three-point function (4.3). The technical details are summarized in appendices A and B.

4.1.1 Outline of the computations

The first goal is to evaluate all the CFT correlation functions in the expansions (4.2) and (4.3) at the leading order in λ, at all orders in g_3 and up to the first order in the derivative couplings, following the strategy given in section 3.3. Namely, starting from the AdS action (3.18), we

1) evaluate all Witten diagrams for the CFT correlation functions in (4.2) and (4.3) in our parameter regime,

2) substitute the results of Step 1) back into the expansions (4.2) and (4.3), and carry out the summations keeping the condition $\bar{\phi}k^{-\lambda} \gtrsim \lambda$ in mind,

3) finally apply the replacement (3.20) to obtain correlation functions of the perturbed CFT.

Step 1) seems intractable apparently, but actually the enumeration of the diagrams is simplified in our parameter region stated in section 3.2. First, we only need to take into account the cubic coupling g_3 out of the slow-roll potential because it dominates over higher-point couplings. Second, diagrams with two or more derivative couplings are subleading thanks to the conditions (3.15) on the derivative couplings. These conditions on the model parameters enable us to complete the computation of relevant diagrams. The detail of Step 1) is given in appendix A. Then, in Step 2), we obtain integral representations of the full two-point and three-point functions after the summations. Remarkably, these integral expressions have very compact structures with what we call "effective bulk-boundary propagators". As explained in more detail shortly, they are bulk-boundary propagators "dressed" with zero-momentum propagators associated with the operator $O_0(\mathbf{0})$. The result of Step 3) is given in appendix B.3.

In the rest of this subsection we explain these results and their consequences more concretely: first evaluate the contributions to the three-point function without derivative couplings, which we will call the "non-derivative part" of the three-point function, and then evaluate the contributions at the first order in the derivative couplings, which we will call the "α_m-part".

4.1.2 Non-derivative part of the three-point function

Let us first focus on the non-derivative part of the three-point function (4.3). As stated above, this part is contributed by Witten diagrams made up of three bulk-boundary prop-

Figure 4. The effective bulk-boundary propagator is essentially taking all contributions of zero momentum legs (indicated in red). When the bulk point is pulled to the boundary according to (A.15), it is exactly the two-point function of the perturbed CFT.
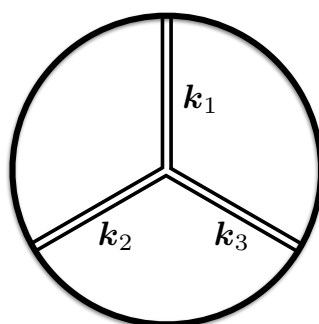
Figure 5. The diagrammatic representation of the integral (4.4). The black double line denotes the effective bulk-boundary propagator $\boldsymbol{K}_{\boldsymbol{k}_i}(z)$.

agators with $\boldsymbol{k}_i$ and an arbitrary number of zero-momentum bulk-boundary propagators, connected by the bulk-bulk propagators and the cubic vertex g_3. We then introduce what we call the effective bulk-boundary propagator schematically as in figure 4. It is essentially a bulk-boundary propagator dressed by zero-momentum propagators with the cubic vertex g_3 (see appendix A for a more precise definition). Notice that this dressing originates from the operator $O_0(\boldsymbol{0})$ in the perturbative expansion (4.3). All the relevant diagrams are now nicely reformulated into the form of figure 5, where three effective bulk-boundary propagators are attached to the cubic coupling g_3. More explicitly,

$$\langle O_0(\boldsymbol{k}_1)O_0(\boldsymbol{k}_2)O_0(\boldsymbol{k}_3)\rangle' \ni -2g_3 \int_0^\infty \frac{dz}{z^4} \boldsymbol{K}_{\boldsymbol{k}_1}(z)\boldsymbol{K}_{\boldsymbol{k}_2}(z)\boldsymbol{K}_{\boldsymbol{k}_3}(z)\,, \qquad (4.4)$$

where $\boldsymbol{K}_{\boldsymbol{q}}(z)$ denotes the effective bulk-boundary propagator of momentum $\boldsymbol{q}$. This is exactly the integral expression of $\langle O_0(\boldsymbol{k}_1)O_0(\boldsymbol{k}_2)O_0(\boldsymbol{k}_3)\rangle_{\mathrm{CFT}}$ with the three bulk-boundary propagators replaced by the effective ones $\boldsymbol{K}_{\boldsymbol{k}_i}(z)$.

Generally speaking, it is quite difficult to evaluate the integral (4.4). However, it turns out to be somewhat tractable under the assumptions $\lambda \ll 1$ and

$$\left(\frac{k_1}{k}\right)^\lambda \sim \left(\frac{k_2}{k}\right)^\lambda \sim \left(\frac{k_3}{k}\right)^\lambda \sim 1\,. \qquad (4.5)$$

where we introduced $k := k_1 + k_2 + k_3$. From an inflationary point of view, the first assumption corresponds to the slow-roll condition as we mentioned earlier. On the other hand, the second one is essentially equivalent to the assumption that the slow-roll parameters are approximately the same at the time of horizon crossing of each mode $\boldsymbol{k}_i$. In appendix B.2.1, we find that the integral (4.4) takes the form,

$$f(\bar{\phi}k^{-\lambda})(k_1^{3-3\lambda} + k_2^{3-3\lambda} + k_3^{3-3\lambda}) \, , \tag{4.6}$$

where $f(\bar{\phi}k^{-\lambda})$ is some function irrelevant to the shape. Actually, because of some combinatorial complications, it seems not straightforward to determine the function $f(\bar{\phi}k^{-\lambda})$ directly. Instead, in the following, we use the consistency relation (3.6), which we already proved on the CFT side for general setups, to find the explicit form of $f(\bar{\phi}k^{-\lambda})$.

Let us start from the right hand side of the consistency relation (3.6). The $\mathcal{O}(\alpha_m^0)$ part of the power spectrum and the spectral tilt were already computed in [8, 17, 21, 24], which gives

$$P_\zeta = \frac{1}{4\pi^2\beta^2(\bar{g}(q))} + \mathcal{O}(\alpha_m) \, , \quad n_s - 1 = -2\beta'(\bar{g}(q)) + \mathcal{O}(\alpha_m) \, . \tag{4.7}$$

Here $\bar{g}(q)$ and $\beta(\bar{g}(q))$ are defined by

$$\bar{g}(q) := \bar{\phi}q^{-\lambda}\left(1 + \frac{g_3}{3}\frac{\bar{\phi}q^{-\lambda}}{\lambda}\right)^{-1} , \tag{4.8}$$

$$\beta(\bar{g}(q)) := -\lambda\bar{g}(q) + \frac{g_3}{3}\bar{g}(q)^2 = -\lambda\bar{\phi}q^{-\lambda}\left(1 + \frac{g_3}{3}\frac{\bar{\phi}q^{-\lambda}}{\lambda}\right)^{-2} . \tag{4.9}$$

As discussed in [21], $\bar{g}(q)$ and $\beta(g)$ may be identified with the coupling for the renormalized operator associated with O_0 and the corresponding beta function. Indeed, $\bar{g}(q)$ flows from UV to IR as

$$0 \leq \bar{g}(q) \leq \frac{3\lambda}{g_3} \, , \tag{4.10}$$

as expected from our inflationary setup. We may also see that β is at most of the order λ^2 along the flow. On the other hand, the left hand side of eq. (3.6) in the squeezed limit reads
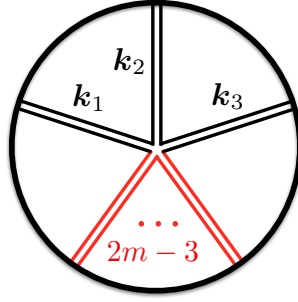
$$-2\lambda + \lambda\bar{\phi}\frac{\text{Re}\langle O_0(\boldsymbol{0})O_0(\boldsymbol{k}_2)O_0(-\boldsymbol{k}_2)\rangle'}{\text{Re}\langle O_0(\boldsymbol{k}_2)O_0(-\boldsymbol{k}_2)\rangle'} = -2\lambda - \frac{2(\lambda\bar{\phi}k^{-\lambda})^3 f(\bar{\phi}k^{-\lambda})}{\beta(\bar{g}(k))^2} \, . \tag{4.11}$$

Here we used the approximation (4.5) and the two-point function,

$$\langle O_0(\boldsymbol{q})O_0(-\boldsymbol{q})\rangle' = -\frac{\beta(\bar{g}(q))^2}{(\lambda\bar{\phi})^2}q^3 + \mathcal{O}(\alpha_m) \, , \tag{4.12}$$

which follows from the result in [8, 17, 21, 24]. The consistency relation (3.6) then implies

$$f(\bar{\phi}k^{-\lambda}) = -\left(\lambda + \beta'(\bar{g}(k))\right)\beta(\bar{g}(k))^2(\lambda\bar{\phi}k^{-\lambda})^{-3} = -\frac{2g_3}{3\lambda}\left(1 + \frac{g_3}{3}\frac{\bar{\phi}k^{-\lambda}}{\lambda}\right)^{-5} . \tag{4.13}$$

Figure 6. The diagrammatic representation of the integral (4.14). The red double line represents the effective zero-momentum bulk-boundary propagator $\boldsymbol{E}(z)$.

4.1.3 α_m-part of the three-point function

We next move on to the α_m-part of the three-point function (4.3). This part is contributed by all diagrams made up of three bulk-boundary propagators with with $\boldsymbol{k}_i$ and an arbitrary number of zero-momentum bulk-boundary propagators, connected by the bulk-bulk propagators, the cubic vertex g_3 and only one derivative coupling. Let us look at the diagrams with one α_m. Similarly to the non-derivative case, all the relevant diagrams are nicely reformulated in terms of effective propagators as in figure 6. Here, the new ingredient is the effective zero-momentum bulk-boundary propagator, i.e., the red double line in the figure. It is again dressed by zero-momentum propagators with the cubic vertex g_3 (see appendix A for more details). More explicitly, the integral representation of the α_m-contribution to the three-point function (4.3) is given by

$$\langle O_0(\boldsymbol{k}_1)O_0(\boldsymbol{k}_2)O_0(\boldsymbol{k}_3)\rangle' \tag{4.14}$$

$$\ni \sum_{m \geq 2} \frac{2m(2m-2)}{2^m} \alpha_m \int_0^\infty dz z^{2m-4} \Big\{ (2m-1) \boldsymbol{K}'_{\boldsymbol{k}_1}(z) \boldsymbol{K}'_{\boldsymbol{k}_2}(z) \boldsymbol{K}'_{\boldsymbol{k}_3}(z) \boldsymbol{E}'(z)^{2m-3}$$

$$- \Big(\boldsymbol{k}_1.\boldsymbol{k}_2 \boldsymbol{K}_{\boldsymbol{k}_1}(z) \boldsymbol{K}_{\boldsymbol{k}_2}(z) \boldsymbol{K}'_{\boldsymbol{k}_3}(z) \boldsymbol{E}'(z)^{2m-3} + (231) + (312) \Big) \Big\},$$

where $\boldsymbol{E}(z)$ denotes the zero-momentum effective bulk-boundary propagator. For the derivation, see appendix A.4. This is exactly the integral expression of $\langle O_0(\boldsymbol{k}_1)O_0(\boldsymbol{k}_2)\cdot$ $\cdot O_0(\boldsymbol{k}_3)O_0(\boldsymbol{0})^{2m-3}\rangle_{\text{CFT}}$ for each m, with the three bulk-boundary propagators replaced by the effective ones $\boldsymbol{K}_{\boldsymbol{k}_i}(z)$ and $(2m-3)$ zero-momentum propagators replaced by the effective ones $\boldsymbol{E}(z)$.

Surprisingly, it turns out that the assumption $\lambda \ll 1$ drastically simplifies our computation. In appendix B we show that the following approximations may be used in the integral (4.14):

$$\boldsymbol{K}_{\boldsymbol{k}_i}(z) \simeq \left(1 + \frac{g_3 \bar{\phi} k^{-\lambda}}{3\lambda} \right)^{-2} \mathcal{K}_{\boldsymbol{k}_i}(z), \tag{4.15}$$

$$\boldsymbol{K}'_{\boldsymbol{k}_i}(z) \simeq \left(1 + \frac{g_3 \bar{\phi} k^{-\lambda}}{3\lambda} \right)^{-2} \mathcal{K}'_{\boldsymbol{k}_i}(z), \tag{4.16}$$

$$\boldsymbol{E}'(z) \simeq \left(1 + \frac{g_3 \bar{\phi} k^{-\lambda}}{3\lambda} \right)^{-2} \left[-\bar{\phi} \mathcal{K}'_{\boldsymbol{0}}(z) \right], \tag{4.17}$$

– 19 –

where $\mathcal{K}_{\boldsymbol{q}}(z)$ is the standard (undressed) bulk-boundary propagator,

$$\mathcal{K}_{\boldsymbol{q}}(z) = \frac{q^{(3/2)-\lambda}z^{3/2}}{2^{(1/2)-\lambda}\Gamma((3/2)-\lambda)}K_{(3/2)-\lambda}(qz)\,. \tag{4.18}$$

Interestingly, all the ingredients of the integral (4.14) have the same z-independent prefactor,

$$\left(1 + \frac{g_3\bar{\phi}k^{-\lambda}}{3\lambda}\right)^{-2} = \frac{\beta(\bar{g}(k))}{-\lambda\bar{\phi}k^{-\lambda}}\,, \tag{4.19}$$

which goes to unity in the UV limit $k \to \infty$. As a result, the shape function takes a form quite similar to the UV results (3.23)–(3.25). By performing the integral (4.14), we have

$$\langle O_0(\boldsymbol{k}_1)O_0(\boldsymbol{k}_2)O_0(\boldsymbol{k}_3)\rangle'\big|_{\alpha_m^1} = -4k_1k_2k_3\frac{\beta(\bar{g}(k))^2}{(\lambda\bar{\phi})^3}\mathcal{F}\left(\frac{k_1}{k_3},\frac{k_2}{k_3}\right)\,, \tag{4.20}$$

with the shape function $\mathcal{F}(k_1/k_3, k_2/k_3)$ defined by

$$\mathcal{F}\left(\frac{k_1}{k_3},\frac{k_2}{k_3}\right) = \left[-\frac{4}{3}X^2 P_{XXX}\frac{3k_1k_2k_3}{2(k_1+k_2+k_3)^3} + 2XP_{XX}G(k_1,k_2,k_3)\right]_{X=\beta(\bar{g}(k))^2/2}\,. \tag{4.21}$$

Here we used the approximations $\lambda \ll 1$ and (4.5). Also notice that all the scale-dependence appears through $X = \beta(\bar{g}(k))^2/2$.

Before stating the final result for the inflationary bispectrum, we would like to make some technical comments. After the computation of the integral (4.14), one may wonder why the computation here was simpler than the one for the non-derivative part. In particular, one may wonder why we cannot use the approximations (4.15)–(4.17) for the non-derivative contribution. Actually, the integrals (4.4) and (4.14) have a different behavior around $z = 0$. First, the leading contribution of the latter integral is regular around $z = 0$ essentially because α_m's are derivative interactions. We can therefore take the $\lambda \to 0$ limit of the integrand before performing the integral. On the other hand, the former is singular for $\lambda \ll 1$, so that we need to perform an analytic continuation of λ. Because of this analytic continuation, we cannot take the $\lambda \to 0$ limit before performing the integral. Essentially, such a difference makes the computation in this subsection simpler compared with the non-derivative part. More details will be discussed in appendix B.

4.1.4 Final result

We now compute the inflationary bispectrum using the obtained deformed QFT correlators. So far, we have computed the three-point function $\langle O_0(\boldsymbol{k}_1)O_0(\boldsymbol{k}_2)O_0(\boldsymbol{k}_3)\rangle'$ up to the first order in α_m. Also, by evaluating the second integral of the right hand side of (B.27), we may show that the $\mathcal{O}(\alpha_m)$ correction to the two-point function $\langle O_0(\boldsymbol{q})O_0(-\boldsymbol{q})\rangle'$ scales as $\sim \alpha_m\lambda^{4(m-1)}$, which is subdominant under the condition (3.15). All in all, the leading contribution to the normalized bispectrum is given by

$$\frac{\langle\zeta(\boldsymbol{k}_1)\zeta(\boldsymbol{k}_2)\zeta(\boldsymbol{k}_3)\rangle'}{\langle\zeta(\boldsymbol{k}_1)\zeta(-\boldsymbol{k}_1)\rangle'\langle\zeta(\boldsymbol{k}_2)\zeta(-\boldsymbol{k}_2)\rangle'} = \beta'(\bar{g}(k))\left(1+\left(\frac{k_1}{k_3}\right)^3+\left(\frac{k_2}{k_3}\right)^3\right) + \frac{4k_1k_2k_3}{k_2^3}\mathcal{F}\left(\frac{k_1}{k_3},\frac{k_2}{k_3}\right)\,. \tag{4.22}$$

4.2 Comparison with inflationary results

In this subsection, we compare the result (4.22) from the dual QFT with the result on the inflation side. For this we first relate the coupling $\bar{g}$ (4.8) with the inflaton. The coupling $\bar{g}$ satisfies

$$\frac{d\bar{g}(k)}{d\ln k} = \beta(\bar{g}(k)) = -\lambda\bar{g}(k) + \frac{g_3}{3}\bar{g}^2(k). \tag{4.23}$$

On the inflation side, the time derivative of the inflaton trajectory $\phi_c(t)$ can be written in terms of the inflaton trajectory ϕ_c itself as[12]

$$\dot{\phi}_c = -\lambda\phi_c + \frac{g_3}{3}\phi_c^2 + \mathcal{O}(\alpha_m). \tag{4.24}$$

This equation holds at any time, especially at the horizon crossing $t_*(k)$ satisfying $k = aH(t_*(k))$. Comparing (4.23) and (4.24), we can identify the running coupling $\bar{g}(k)$ at the leading order in λ with the inflaton at the horizon exit $\phi_c(t_*(k))$ up to α_m-corrections,

$$\phi_c(t_*(k)) = \bar{g}(k) + \mathcal{O}(\alpha_m). \tag{4.25}$$

Let us apply this identification to the bispectrum directly computed on the inflation side [28]. In our parameter regime, the leading contribution is

$$\frac{\langle\zeta(\boldsymbol{k}_1)\zeta(\boldsymbol{k}_2)\zeta(\boldsymbol{k}_3)\rangle'}{\langle\zeta(\boldsymbol{k}_1)\zeta(-\boldsymbol{k}_1)\rangle'\langle\zeta(\boldsymbol{k}_2)\zeta(-\boldsymbol{k}_2)\rangle'}$$

$$= \frac{\eta}{2}\left(1 + \left(\frac{k_1}{k_3}\right)^3 + \left(\frac{k_2}{k_3}\right)^3\right)$$

$$+ \frac{4k_1k_2k_3}{k_3^3}\left[\left(\frac{1}{c_s^2} - 1 - 2\frac{\Lambda}{\Sigma}\right)\frac{3k_1k_2k_3}{2(k_1+k_2+k_3)} + \left(\frac{1}{c_s^2} - 1\right)G(k_1,k_2,k_3)\right], \tag{4.26}$$

where the parameters Λ, Σ are defined as [28]

$$\Lambda := XP_{XX} + \frac{2}{3}X^2P_{XXX}, \quad \Sigma := P_X + 2XP_{XX}. \tag{4.27}$$

Here these parameters and the sound speed are defined with $X = \frac{1}{2}\dot{\phi}_c^2$. First the slow-roll parameter η becomes $\eta = 2\beta'$. Next, the remaining parameters become, at the leading order in the derivative couplings,

$$X = \frac{1}{2}\dot{\phi}_c^2 \simeq \frac{1}{2}\beta(\bar{g}(k))^2,$$

$$\frac{1}{c_s^2} - 1 = \frac{2XP_{XX}}{P_X} \simeq 2XP_{XX},$$

$$\frac{1}{c_s^2} - 1 - \frac{2\Lambda}{\Sigma} = \frac{2XP_{XX}}{P_X} - 2\frac{XP_{XX} + \frac{2}{3}X^2P_{XXX}}{P_X + 2XP_{XX}} \simeq -\frac{4}{3}X^2P_{XXX}, \tag{4.28}$$

where $\simeq$ stands for the equality up to the leading order in α_m. Applying these results to (4.26), we find it exactly coincides with (4.22), as desired.

---

[12]This is derived by writing $\dot{\phi}_c$ in terms of ϕ_c. See [21] for the detail for a general slow-roll potential.

5 Summary and outlook

In this paper, we applied conformal perturbation techniques to holographically compute the bispectrum of a generalized single-field inflation model containing derivative couplings. Correlation functions of the reference UV CFT were computed via the dS/CFT correspondence. Using them, we first computed correlation functions of a relevantly deformed CFT perturbatively around the UV fixed point, and obtained a blue tilted power spectrum as well as a bispectrum of the correct shape. Then, by taking into account all-order conformal perturbations to reach the IR region of the RG flow, we reproduced the bispectrum up to first order in the derivative couplings at scales where the power spectrum is red tilted.

We would like to end this paper with several promising future directions. First, our analysis in the present paper was perturbative in the derivative couplings. While our result is exact to all orders in the cubic coupling g_3, it is valid only around the parameter region with $c_s^2 \sim 1$. It would be interesting to generalize our findings to the small sound speed case where $c_s^2 \ll 1$. Another interesting direction will be to extend our results to quasi single-field inflation [42–44] (which contains massive fields in addition to the inflaton), especially in connection to the "cosmological collider physics" program [45]. The CFT viewpoint will be useful in understanding various soft limit properties of the inflationary correlators. Furthermore, recent developments in higher dimensional CFT, such as the conformal bootstrap approach,[13] may give us additional handles to derive inflationary non-Gaussianities. We expect such technical advances, together with conformal perturbation theory and holography that we exploited in this paper, would shed new light on the structure of primordial spectra. We hope to report our progress in these directions elsewhere in the near future.

---

[13]See, e.g., [46, 47] for application of the conformal bootstrap approach to non-unitary CFTs, which will be relevant in the context of dS/CFT.

A Correlation functions from AdS

This and the next appendices will give a detailed account of computing CFT correlation functions from an AdS action. In this appendix, we give a classical solution to the equation of motion of the AdS action perturbatively, compute their derivatives and use them to write down the correlation functions of our interest. See the appendix B of [21] for a nice review for the canonical kinetic term case. This section is its extension to the case with derivative couplings.

A.1 Review of holographic computations in AdS

The bulk AdS action of our interest is

$$S_{\text{AdS}} = \int d^4x \sqrt{G} \left[\frac{1}{2}(\partial\Phi)^2 + \frac{m^2}{2}\Phi^2 - \frac{g_3}{3}\Phi^3 + \sum_{m \geq 2} \frac{a_m}{2^m}(\partial\Phi)^{2m} \right], \tag{A.1}$$

where $(\partial\Phi)^2 := G^{MN}\partial_M\Phi\partial_N\Phi$ and G_{MN} is the Euclidean four-dimensional AdS metric $ds^2 = R_{\text{AdS}}^2 z^{-2}(dz^2 + d\boldsymbol{x}^2)$. The equation of motion of Φ is

$$-G^{-1/2}\partial_M(G^{1/2}\partial^M\Phi) + m^2\Phi - g_3\Phi^2 - \sum_{m \geq 2} \frac{a_m}{2^m}G^{-1/2}\partial_M(G^{1/2}\partial^M\Phi(\partial\Phi)^{2(m-1)}) = 0. \tag{A.2}$$

Let us introduce a parameter ν and formally expand Φ in ν as $\Phi = \sum_{n=1}^{\infty} \nu^n \Phi_n$. Then the equations of motion for Φ_n read

$$0 = \mathcal{D}\Phi_1, \tag{A.3}$$

$$0 = \mathcal{D}\Phi_2 - g_3\Phi_1^2, \tag{A.4}$$

$$0 = \mathcal{D}\Phi_n - g_3 \sum_{\substack{a+b=n \\ a,b \geq 1}} \Phi_a\Phi_b$$

$$- \sum_{m \geq 2} \frac{2ma_m}{2^m} \sum_{\substack{a+\sum_i(b_i+c_i)=n \\ a,b_i,c_i \geq 1}} G^{-1/2}\partial_M(G^{1/2}\partial^M\Phi_a(\partial_N\Phi_{b_i}\partial^N\Phi_{c_i})^{m-1}), \tag{A.5}$$

where the third equation is for $n \geq 3$, and $\mathcal{D}$ is the differential operator

$$\mathcal{D}\Phi := -G^{-1/2}\partial_M(G^{1/2}\partial^M\Phi) + m^2\Phi. \tag{A.6}$$

We solve the first equation of motion (A.3) by

$$\Phi_1(X) = \int_{\boldsymbol{x}} \mathcal{K}_X(\boldsymbol{x})\varphi_{[0]}(\boldsymbol{x}), \tag{A.7}$$

where $\varphi_{[0]}(\boldsymbol{x})$ is the boundary field, $X = (z, \boldsymbol{y})$ denotes a bulk point, and we introduced the bulk-boundary propagator $\mathcal{K}_X(\boldsymbol{x})$, which satisfies $\mathcal{D}_X\mathcal{K}_X(\boldsymbol{x}) = 0$. We will use its three-dimensional momentum expression

$$\mathcal{K}_{\boldsymbol{q}}(z) := \frac{q^{(3/2)-\lambda}z^{3/2}}{2^{(1/2)-\lambda}\Gamma((3/2)-\lambda)}K_{(3/2)-\lambda}(qz), \quad R_{\text{AdS}}^2 m^2 = \lambda(\lambda - 3), \tag{A.8}$$

which is defined by

$$\mathcal{K}_{(z,\boldsymbol{y})}(\boldsymbol{x}) = \int \frac{d^3q}{(2\pi)^3} e^{i\boldsymbol{q}.(\boldsymbol{x}-\boldsymbol{y})} \mathcal{K}_{\boldsymbol{q}}(z).$$

Here the normalization factor in $\mathcal{K}_{\boldsymbol{q}}$ is fixed such that $\mathcal{K}_{\boldsymbol{q}}(z) \to z^\lambda$ as $z \to 0$. To solve the remaining equations of motion (A.4) and (A.5), we introduce the Green's function $\mathcal{G}(z,\boldsymbol{x};z',\boldsymbol{x}')$, called the bulk-bulk propagator, as the solution to the free equation of motion with a delta-function source

$$R_{\text{AdS}}^2 \mathcal{D}_z \mathcal{G}(z,\boldsymbol{x};z',\boldsymbol{x}') = z^4 \delta(z-z')\delta^3(\boldsymbol{x}-\boldsymbol{x}'). \tag{A.9}$$

The overall R_{AdS}^2 on the left hand side is introduced so that the R_{AdS}^2-dependence only comes from the mass in the form $R_{\text{AdS}}^2 m^2$. Its three-dimensional momentum space $\mathcal{G}_{\boldsymbol{q}}(z,z')$ reads

$$\mathcal{G}_{\boldsymbol{q}}(z,z') = \begin{cases} (zz')^{3/2} K_{\frac{3}{2}-\lambda}(qz) I_{\frac{3}{2}-\lambda}(qz') & z > z', \\ (zz')^{3/2} I_{\frac{3}{2}-\lambda}(qz) K_{\frac{3}{2}-\lambda}(qz') & z' > z, \end{cases} \tag{A.10}$$

which is defined by

$$\mathcal{G}(z,\boldsymbol{x};z',\boldsymbol{x}') = \int \frac{d^3q}{(2\pi)^3} e^{i\boldsymbol{q}.(\boldsymbol{x}-\boldsymbol{x}')} \mathcal{G}_{\boldsymbol{q}}(z,z').$$

The solutions to the equations of motion (A.4) and (A.5) then read

$$\Phi_{2,X} = g_3 R_{\text{AdS}}^{-2} \int_{X'} \mathcal{G}_{XX'} \Phi_{1,\boldsymbol{X}'} \Phi_{1,\boldsymbol{X}'}, \tag{A.11}$$

$$\Phi_{n,X} = g_3 R_{\text{AdS}}^{-2} \int_{X'} \mathcal{G}_{XX'} \sum_{\substack{a+b=n \\ a,b\geq 1}} \Phi_{a,X'} \Phi_{b,X'} + \sum_{m\geq 2} \frac{2m}{2^m} a_m R_{\text{AdS}}^{2(m-5)} \tag{A.12}$$

$$\times \int_{X'} \mathcal{G}_{XX'} \sum_{\substack{a+\sum_i(b_i+c_i)=n \\ a,b,c\geq 1}} z'^4 \partial'_M \left[z'^{2(m-2)} \partial'_M \Phi_{a,X'} (\partial'_N \Phi_{b_i,X'} \partial'_N \Phi_{c_i,X'})^{m-1} \right],$$

where each of the indices M, N is summed over $z, \boldsymbol{x}$.[14] Just for notational simplicity, we introduced the abbreviations: for $\Phi_{a,X} = \Phi_a(z,\boldsymbol{x})$, $\mathcal{G}_{XX'} = \mathcal{G}(z,\boldsymbol{x};z',\boldsymbol{x}')$, $G_z^{MN} = G^{MN}(z), \partial'_M = \frac{\partial}{\partial z'^M}$ and $\int_{X'} := \int \frac{dz'}{z'^4} \int d^3\boldsymbol{x}'$.

AdS/CFT dictionary. To describe the AdS/CFT correspondence precisely, we use the asymptotic behavior of Φ as $z \to 0$, which is given as the sum of two power series

$$\Phi(z) = z^\lambda \left(\varphi_{[0]} + z^2 \varphi_{[2]} + \cdots \right) + z^{3-\lambda} \left(\varphi_{[3-2\lambda]} + z^2 \varphi_{[5-2\lambda]} \cdots \right). \tag{A.13}$$

The holographic dictionary is to identify $\varphi_{[3-2\lambda]}$ with the 1-point function in the presence of the boundary field $\varphi_{[0]}$ up to contact terms [48],

$$\langle O_0 \rangle_{\text{s}} = -R_{\text{AdS}}^2 (3-2\lambda) \varphi_{[3-2\lambda]}. \tag{A.14}$$

---

[14]Note that the integral measure also involves R_{AdS}^4 from $\sqrt{G}$, which, however, is irrelevant to the flip (3.20).

One can extract $\varphi_{[3-2\lambda]}$ from (A.12) by expanding $\mathcal{G}_{XX'}$ at $z \to 0$, $z < z'$,

$$\mathcal{G}_{\boldsymbol{q}}(z, z') = \frac{1}{3 - 2\lambda}\mathcal{K}_{\boldsymbol{q}}(z')z^{3-\lambda} + \mathcal{O}(z^{5-\lambda}), \tag{A.15}$$

such that the contribution of $\Phi_{n,X}$ to $\langle O_0 \rangle_s$ are obtained by replacing $\mathcal{G}_{\boldsymbol{q}}(z, z')$ by $\mathcal{K}_{\boldsymbol{q}}(z')$ in (A.12). Correlation functions are obtained by taking derivatives with respect to $-\varphi_{[0]}$

$$\langle O_0(\boldsymbol{k}_1) \ldots O_0(\boldsymbol{k}_n) \rangle = (-)^{n-1}\frac{\delta^{n-1}\langle O_0(\boldsymbol{k}_1)\rangle_s}{\delta\varphi_{[0]}(-\boldsymbol{k}_2)\ldots\delta\varphi_{[0]}(-\boldsymbol{k}_n)}\bigg|_{\varphi_{[0]}=0}. \tag{A.16}$$

Note that the correlation functions thus obtained are those of CFT_3 dual to AdS_4. We can see from (A.7), (A.11) and (A.12) that Φ_n contains n source fields $\varphi_{[0]}$. They can be drawn as Witten diagrams with the bulk-bulk propagator $\mathcal{G}$ and the bulk-boundary propagator $\mathcal{K}$ and all the combinatorial factors are contained in Φ_n. Correlation functions in our perturbed CFT are expressed as an infinite sum of the CFT correlators, for instance,

$$\langle O_0(\boldsymbol{k}_1)O_0(\boldsymbol{k}_2)\rangle' = \sum_{n=0}^{\infty}\frac{(-\bar{\phi})^n}{n!}\langle O_0(\boldsymbol{k}_1)O_0(\boldsymbol{k}_2)O_0(\boldsymbol{0})^n\rangle'_{\text{CFT}}. \tag{A.17}$$

Since all UV CFT correlation functions contribute at the same order at the IR, we need n-point functions for general n in which two or three operators have nonzero momenta and others have zero momentum. To evaluate them, we first take the n-th, $(n-1)$-th, and $(n-2)$-th derivatives of Φ_n with respect to the boundary fields with zero momentum. Moreover, we will evaluate the correlation functions to all orders in g_3 and to first order in a_m. We will finally find that the two-point and three-point functions can be compactly written in terms of the effective bulk-boundary propagators, which can be depicted as Witten diagrams in figure 5 plus figure 6. Diagrammatic representation of the effective bulk-boundary propagators will be given in figure 4 and 8.

For later convenience, we first decompose Φ_n as

$$\Phi_n = \Phi_n^{(g_3)} + \sum_{m \geq 2}\Phi_n^{(a_m)}. \tag{A.18}$$

Here $\Phi_n^{(g_3)}$ has no derivative couplings a_m while $\Phi_n^{(a_m)}$ has only one a_m for each m.

Recovering the AdS radius. From now on, we will set $R_{\text{AdS}} = 1$ for simplicity. We can recover the R_{AdS}^2 dependence by applying the following replacement

$$g_3 \longrightarrow R_{\text{AdS}}^{-2}g_3, \quad a_m \longrightarrow R_{\text{AdS}}^{2(m-5)}a_m, \quad \langle OO\ldots\rangle_{\text{AdS}} \longrightarrow R_{\text{AdS}}^2\langle OO\ldots\rangle_{\text{AdS}}. \tag{A.19}$$
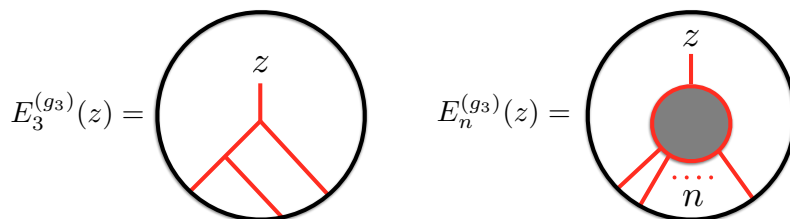
A.2 Properties of $\Phi_n^{(g_3)}$

Keeping the correlation functions of our interest in mind, we introduce

$$C_{n,\boldsymbol{k}_1,\boldsymbol{k}_2}^{(g_3)}(z) = \frac{2}{(n-2)!(2g_3)^{n-1}}\frac{\delta^n\Phi_n^{(g_3)}(z, \boldsymbol{k}_3)}{\delta\varphi_{[0]}(-\boldsymbol{k}_1)\delta\varphi_{[0]}(-\boldsymbol{k}_2)\delta\varphi_{[0]}(\boldsymbol{0})^{n-2}}, \tag{A.20}$$

$$K_{n,\boldsymbol{k}_1}^{(g_3)}(z) = \frac{1}{(n-1)!(2g_3)^{n-1}}\frac{\delta^n\Phi_n^{(g_3)}(z, \boldsymbol{k}_2)}{\delta\varphi_{[0]}(-\boldsymbol{k}_1)\delta\varphi_{[0]}(\boldsymbol{0})^{n-1}}, \tag{A.21}$$

$$E_n^{(g_3)}(z) = \frac{1}{n!(2g_3)^{n-1}}\frac{\delta^n\Phi_n^{(g_3)}(z, \boldsymbol{0})}{\delta\varphi_{[0]}(\boldsymbol{0})^n}, \tag{A.22}$$

Figure 7. Diagrams for $E_n^{(g_3)}$. The index n is the number of the zero-momentum bulk-boundary propagators.

where we have omitted momentum-conserving delta function $(2\pi)^3\delta(\sum \boldsymbol{k}_i)$.[15] Here we make a comment on the meaning of the normalizations above. We will shortly find that the recursion relations for $C^{(g_3)}, K^{(g_3)}, E^{(g_3)}$ involve no coupling constant g_3. This implies that the $C^{(g_3)}, K^{(g_3)}, E^{(g_3)}$ are all independent of g_3, so that the normalizations above tell us the exact g_3-dependence of the above three derivatives of $\Phi_n^{(g_3)}$.

Taking derivatives of (A.7), (A.11) and (A.12), we find the recursion relations for $E_n^{(g_3)}$

$$E_1^{(g_3)}(z) = \mathcal{K}_{\boldsymbol{0}}(z), \tag{A.23}$$

$$E_n^{(g_3)}(z) = \frac{1}{2}\int_{z'}\sum_{\substack{a+b=n \\ a,b\geq 1}}\mathcal{G}_{\boldsymbol{0}}(z,z')E_a^{(g_3)}(z')E_b^{(g_3)}(z'). \quad (n\geq 2) \tag{A.24}$$

This can be depicted as figure 7.

The recursion relations for $K_n^{(g_3)}$ read

$$K_{1,\boldsymbol{k}}^{(g_3)}(z) = \mathcal{K}_{\boldsymbol{k}}(z), \tag{A.25}$$

$$K_{n,\boldsymbol{k}}^{(g_3)}(z) = \int_{z'}\sum_{\substack{a+b=n \\ a,b\geq 1}}\mathcal{G}_{\boldsymbol{k}}(z,z')E_a^{(g_3)}(z')K_{b,\boldsymbol{k}}^{(g_3)}(z'). \quad (n\geq 2) \tag{A.26}$$

In terms of $E^{(g_3)}$, it reads,

$$K_{n,\boldsymbol{k}}^{(g_3)}(z) = \sum_{\substack{p\geq 0 \\ n_1+...+n_p=n-1 \\ 1\leq n_1,...,n_p\leq n-1}}\int_{z_1,...,z_p}\mathcal{G}_{\boldsymbol{k}}(z,z_1)E_{n_1}^{(g_3)}(z_1)\mathcal{G}_{\boldsymbol{k}}(z_1,z_2)E_{n_2}^{(g_3)}(z_2)\cdots\mathcal{G}_{\boldsymbol{k}}(z_{p-1},z_p)E_{n_p}^{(g_3)}(z_p)\mathcal{K}_{\boldsymbol{k}}(z_p). \tag{A.27}$$

The summation symbol $\sum_{p\geq 0}\sum_{n_1+...+n_p=n-1,1\leq n_1,...,n_p\leq n-1}$ means that the sum over all possible decompositions of $n-1$ into a sum of integers no less than 1. In the $n=1$ case, this decomposition does not exist, namely $p=0$, consistent with (A.25). Diagrammatically, it simply means attaching $(n-1)$ zero momentum legs to the bulk-boundary propagator using the g_3 vertex.

---

[15]More concretely, for (A.20), it holds that $\boldsymbol{k}_1 + \boldsymbol{k}_2 + \boldsymbol{k}_3 = \boldsymbol{0}$, and for (A.20), it holds that $\boldsymbol{k}_1 + \boldsymbol{k}_2 = \boldsymbol{0}$.

The recursion relations for $C_n^{(g_3)}$ read

$$C_{2,\boldsymbol{k}_1,\boldsymbol{k}_2}^{(g_3)}(z) = \int_{z'} \mathcal{G}_{\boldsymbol{k}_1+\boldsymbol{k}_2}(z,z') K_{1,\boldsymbol{k}_1}^{(g_3)}(z') K_{1,\boldsymbol{k}_2}^{(g_3)}(z'), \tag{A.28}$$

$$C_{n,\boldsymbol{k}_1,\boldsymbol{k}_2}^{(g_3)}(z) = \int_{z'} \sum_{\substack{a+b=n \\ a,b\geq 1}} \mathcal{G}_{\boldsymbol{k}_1+\boldsymbol{k}_2}(z,z') \left[E_a^{(g_3)}(z') C_{b,\boldsymbol{k}_1,\boldsymbol{k}_2}^{(g_3)}(z') + K_{a,\boldsymbol{k}_1}^{(g_3)}(z') K_{b,\boldsymbol{k}_2}^{(g_3)}(z') \right]. \quad (n \geq 3) \tag{A.29}$$

It can be expressed as

$$C_{n,\boldsymbol{k}_1,\boldsymbol{k}_2}^{(g_3)}(z) = \int_{X'} \sum_{\substack{a+b+c=n \\ a\geq 0,\ b,c\geq 1}} G_{a,\boldsymbol{k}_1+\boldsymbol{k}_2}(z,z') K_{b,\boldsymbol{k}_1}^{(g_3)}(z') K_{c,\boldsymbol{k}_2}^{(g_3)}(z'), \tag{A.30}$$

where we defined for $n \geq 0$

$$G_{n,\boldsymbol{k}}(z,z') :=$$
$$\sum_{\substack{p\geq 0 \\ n_1+\ldots+n_p=n \\ 1\leq n_1,\ldots,n_p\leq n}} \int_{z_1,\ldots,z_p} \mathcal{G}_{\boldsymbol{k}}(z,z_1) E_{n_1}^{(g_3)}(z_1) \mathcal{G}_{\boldsymbol{k}}(z_1,z_2) E_{n_2}^{(g_3)}(z_2) \cdots \mathcal{G}_{\boldsymbol{k}}(z_{p-1},z_p) E_{n_p}^{(g_3)}(z_p) \mathcal{G}_{\boldsymbol{k}}(z_p,z'), \tag{A.31}$$

where $G_{0,\boldsymbol{k}}$ is equal to $\mathcal{G}_{\boldsymbol{k}}$. The following figure shows this definition diagrammatically:

A.3 Properties of $\Phi_n^{(a_m)}$

In a similar manner, from $\Phi_n^{(a_m)}$ one can obtain $C_n^{(a_m)}$ with $(n-2)$ zero momentum legs and one a_m vertex, $K_n^{(a_m)}$ with $(n-1)$ zero momentum legs and one a_m vertex, and $E_n^{(a_m)}$ with n zero momentum legs and one a_m vertex. Here we explain the case $m=2$ in detail. The extension to general m is straightforward, though the computations will be a bit more complicated. For instance, the three-point function is derived from $C_{n,\boldsymbol{k}_1,\boldsymbol{k}_2}^{(a_2)}$,

$$C_{n,\boldsymbol{k}_1,\boldsymbol{k}_2}^{(a_2)}(z) := \frac{1}{(n-2)! a_2 (2g_3)^{n-3}} \frac{\delta^n \Phi_n^{(a_2)}(z,\boldsymbol{k}_3)}{\delta\varphi_{[0]}(-\boldsymbol{k}_1)\delta\varphi_{[0]}(-\boldsymbol{k}_2)\delta\varphi_{[0]}(\boldsymbol{0})^{n-2}}$$

$$= -\int_{z'} \sum_{\substack{a+b+c+d=n \\ a\geq 0,\ b,c,d\geq 1}} \partial'_M G_{a,\boldsymbol{k}_1+\boldsymbol{k}_2}(z,z') \Big[\partial'^M E_b^{(g_3)}(z') \partial'_N K_{c,\boldsymbol{k}_1}^{(g_3)}(z') \partial'^N K_{d,\boldsymbol{k}_2}^{(g_3)}(z')$$
$$+ 2\partial'^M K_{b,\boldsymbol{k}_1}^{(g_3)}(z') \partial'_N K_{c,\boldsymbol{k}_2}^{(g_3)}(z') \partial'^N E_d^{(g_3)}(z') \Big]$$

$$
-\int_{z'} \sum_{\substack{a+b+c+d=n\\ a\geq 0,\ b,c,d\geq 1}} \partial'_M G_{a,\boldsymbol{k}_1+\boldsymbol{k}_2}(z,z') \Big[\frac{1}{2}\partial'^M C^{(g_3)}_{b,\boldsymbol{k}_1,\boldsymbol{k}_2}(z')\partial'_N E^{(g_3)}_c(z')\partial'^N E^{(g_3)}_d(z')
$$
$$
+\partial'^M E^{(g_3)}_b(z')\partial'_N E^{(g_3)}_c(z')\partial'^N C^{(g_3)}_{d,\boldsymbol{k}_1,\boldsymbol{k}_2}(z')\Big]
$$
$$
+\int_{z'} \sum_{\substack{a+b+c=n\\ a\geq 0,\ b,c\geq 1}} G_{a,\boldsymbol{k}_1+\boldsymbol{k}_2}(z,z')\left\{K^{(g_3)}_{b,\boldsymbol{k}_1}(z')K^{(a_2)}_{c,\boldsymbol{k}_2}(z')+C^{(g_3)}_{b,\boldsymbol{k}_1,\boldsymbol{k}_2}(z')E^{(a_2)}_c(z')\right\},
$$
$$
\tag{A.32}
$$

and the two-point function is derived from $K^{(a_2)}_{n,\boldsymbol{k}_1}$,

$$
K^{(a_2)}_{n,\boldsymbol{k}_1}(z) := \frac{1}{(n-1)!a_2(2g_3)^{n-3}}\frac{\delta^n \Phi^{(a_2)}_n(z,\boldsymbol{k}_2)}{\delta\varphi_{[0]}(-\boldsymbol{k}_1)\delta\varphi_{[0]}(\mathbf{0})^{n-1}}
$$
$$
= -\int_{z'} \sum_{\substack{a+b+c+d=n\\ a\geq 0,\ b,c,d\geq 1}} \partial'_M G_{a,\boldsymbol{k}_1}(z,z') \Big[\partial'^M K^{(g_3)}_{b,\boldsymbol{k}_1}(z')\partial'_N E^{(g_3)}_c(z')\partial'^N E^{(g_3)}_d(z')
$$
$$
+2\partial'^M E^{(g_3)}_b(z')\partial'_N E^{(g_3)}_c(z')\partial'^N K^{(g_3)}_{d,\boldsymbol{k}_1}(z')\Big]
$$
$$
+\int_{z'} \sum_{\substack{a+b+c=n\\ a\geq 0,\ b,c\geq 1}} G_{a,\boldsymbol{k}}(z,z')E^{(a_2)}_b(z')K^{(g_3)}_{c,\boldsymbol{k}_1}(z'),
\tag{A.33}
$$

where we introduced $\partial_M E_n = (\partial_z E_n, \mathbf{0})$ and $\partial_M \mathcal{K}_{n,\boldsymbol{q}} = (\partial_z, i\boldsymbol{q})\mathcal{K}_{n,\boldsymbol{q}}(z)$, etc. for momentum space we are working in. Indices are contracted as usual. We omit the expressions for $E^{(a_2)}_n$ since our results will not involve it at the leading order in λ.

Based on the above results, we can now define the effective propagators,

$$
\boldsymbol{E}(z) := \sum_{n=1}^{\infty}(-2g_3)^{n-1}(-\bar{\phi})^n E^{(g_3)}_n(z),
\tag{A.34}
$$

$$
\boldsymbol{K}_{\boldsymbol{q}}(z) := \sum_{n=1}^{\infty}(2g_3\bar{\phi})^{n-1}K^{(g_3)}_{n,\boldsymbol{q}}(z)
$$
$$
= \sum_{p=0}^{\infty}(-2g_3)^p \int_{z_1,\ldots,z_p} \mathcal{G}_{\boldsymbol{q}}(z,z_1)\boldsymbol{E}(z_1)\mathcal{G}_{\boldsymbol{q}}(z_1,z_2)\cdots\boldsymbol{E}(z_p)\mathcal{K}_{\boldsymbol{q}}(z_p),
\tag{A.35}
$$

$$
\widetilde{\boldsymbol{E}}(z) := \sum_{n=1}^{\infty}(-2g_3)^{n-3}(-\bar{\phi})^n a_2 E^{(a_2)}_n(z)
$$
$$
= -a_2 \int_{z'} \partial'_M \boldsymbol{G}_{\mathbf{0}}(z,z')\partial'^M \boldsymbol{E}(z')\partial'_N \boldsymbol{E}(z')\partial'^N \boldsymbol{E}(z'),
\tag{A.36}
$$

$$
\boldsymbol{G}_{\boldsymbol{q}}(z,z') := \sum_{n=0}^{\infty}(2g_3\bar{\phi})^n G_{n,\boldsymbol{q}}(z,z')
$$
$$
= \sum_{p=0}^{\infty}(-2g_3)^p \int_{z_1,\ldots,z_p} \mathcal{G}_{\boldsymbol{q}}(z,z_1)\boldsymbol{E}(z_1)\mathcal{G}_{\boldsymbol{q}}(z_1,z_2)\cdots\boldsymbol{E}(z_p)\mathcal{G}_{\boldsymbol{q}}(z_p,z').
\tag{A.37}
$$

We will only use the bulk-boundary effective propagators $\boldsymbol{E}, \boldsymbol{K}$ explicitly later. Here, we give their diagrammatic representations.
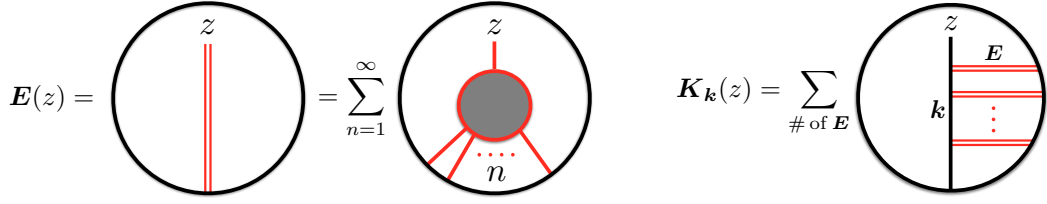
Figure 8. The diagram on the left is the Witten diagram of the effective zero momentum bulk-boundary propagator $\boldsymbol{E}(z)$. The one on the right is the effective bulk-boundary propagator $\boldsymbol{K}_{\boldsymbol{k}}(z)$ in terms of $\boldsymbol{E}$. See also figure 4.

A.4 Correlation functions at all orders

We derive AdS$_4$ integral representations of the two-point and three-point functions using the derivatives of the classical solutions found in the last appendix. In what follows, CFT correlation functions in section A.4.1, A.4.2, B.1 and B.2 are all for CFT dual to AdS, while those defined with CFT dual to dS only appear in section B.3.

A.4.1 Two-point function

The full two-point function can be written as

$$\langle O_0(\boldsymbol{q})O_0(-\boldsymbol{q})\rangle' = \sum_{n=0}^{\infty} \frac{(-\bar{\phi})^n}{n!} \langle O_0(\boldsymbol{q})O_0(-\boldsymbol{q})O_0(\boldsymbol{0})^n\rangle'_{\text{CFT}} \tag{A.38}$$

$$= \left[\sum_{n=0}^{\infty} (2g_3\bar{\phi})^n K_{n+1,\boldsymbol{q}}^{(g_3)}(z) + \sum_{n=2}^{\infty} (-\bar{\phi})^n (-2g_3)^{n-2} a_2 K_{n+1,\boldsymbol{q}}^{(a_2)}(z) \right]_{[3-2\lambda]}.$$

Here the operation $A|_{[3-2\lambda]}$ means picking up the coefficient of $z^{3-\lambda}$-term in the asymptotic form of A as $z \to 0$ and multiplying it by $(3-2\lambda)R_{\text{AdS}}^2$ (to put it practically, replacing every first $\mathcal{G}_{\boldsymbol{q}}(z,z')$ with $\mathcal{K}_{\boldsymbol{q}}(z')$ in the integrals). Diagrammatically, it means pulling the bulk point with coordinate z to the boundary. The first term of (A.38) is just the effective bulk-boundary propagator with the bulk point pulled to the boundary,

$$\sum_{n=0}^{\infty} (2g_3\bar{\phi})^n K_{n+1,\boldsymbol{q}}^{(g_3)}(z) \Big|_{[3-2\lambda]}$$

$$= \boldsymbol{K}_{\boldsymbol{q}}(z) \Big|_{[3-2\lambda]} \tag{A.39}$$

$$= \sum_{p\geq 0} (-2g_3)^p \int_{z_1,\dots,z_p} \mathcal{K}_{\boldsymbol{q}}(z_1)\boldsymbol{E}(z_1)\mathcal{G}_{\boldsymbol{q}}(z_1,z_2)\boldsymbol{E}(z_2)\cdots\mathcal{G}_{\boldsymbol{q}}(z_{p-1},z_p)\boldsymbol{E}(z_p)\mathcal{K}_{\boldsymbol{q}}(z_p),$$

where $p=0$ in the sum is just the CFT two-point function $\langle O_0(\boldsymbol{k})O_0(-\boldsymbol{k})\rangle'_{\text{CFT}}$, we find

$$\langle O_0(\boldsymbol{q})O_0(-\boldsymbol{q})\rangle'$$

$$= \boldsymbol{K}_{\boldsymbol{q}}(z) \Big|_{[3-2\lambda]}$$

$$\quad - a_2 \int_z \partial_M \boldsymbol{K}_{\boldsymbol{q}}(z) \left[\partial^M \boldsymbol{K}_{\boldsymbol{q}}(z)\partial_N \boldsymbol{E}(z)\partial^N \boldsymbol{E}(z) + 2\partial^M \boldsymbol{E}(z)\partial_N \boldsymbol{E}(z)\partial^N \boldsymbol{K}_{\boldsymbol{q}}(z) \right]$$

$$+ 2g_3 a_2 \int_{z,z'} \boldsymbol{K_q}(z)^2 \partial'_M \boldsymbol{G_0}(z,z') \partial'^M \boldsymbol{E}(z') \partial'_N \boldsymbol{E}(z') \partial'^N \boldsymbol{E}(z')$$

$$= \boldsymbol{K_q}(z)\big|_{[3-2\lambda]}$$

$$\qquad - a_2 \int dz \left[3 \partial_z \boldsymbol{K_q}(z) \partial_z \boldsymbol{K_q}(z) \partial_z \boldsymbol{E}(z) \partial_z \boldsymbol{E}(z) - \boldsymbol{q}^2 \boldsymbol{K_q}(z)^2 \partial_z \boldsymbol{E}(z) \partial_z \boldsymbol{E}(z) \right]$$

$$\qquad + \dots . \tag{A.40}$$

Here we introduced the notation $\partial_M \boldsymbol{E} = (\partial_z \boldsymbol{E}, \boldsymbol{0})$ and $\partial_M \boldsymbol{K_q} = (\partial_z, i\boldsymbol{q}) \boldsymbol{K_q}(z)$. Indices are contracted as usual. We omitted the $\mathcal{O}(g_3 a_2)$ term, which turns out to be subleading in λ.

A.4.2 Three-point function

We begin with the identity

$$\langle O_0(\boldsymbol{k}_1) O_0(\boldsymbol{k}_2) O_0(\boldsymbol{k}_3) \rangle'$$

$$= \sum_{n=0}^{\infty} \frac{(-\bar{\phi})^n}{n!} \langle O_0(\boldsymbol{k}_1) O_0(\boldsymbol{k}_2) O_0(\boldsymbol{k}_3) O_0(\boldsymbol{0})^n \rangle'_{\mathrm{CFT}} \tag{A.41}$$

$$= \left[\sum_{n=0}^{\infty} \frac{(-\bar{\phi})^n (-2g_3)^{n+1}}{2} C^{(g_3)}_{n+2, \boldsymbol{k}_2, \boldsymbol{k}_3}(z) + \sum_{n=1}^{\infty} (-\bar{\phi})^n (-2g_3)^{n-1} a_2 C^{(a_2)}_{n+2, \boldsymbol{k}_2, \boldsymbol{k}_3}(z) \right]_{[3-2\lambda]}.$$

Using the recursive relations we found, we can rewrite the three-point function (A.41) as

$$\langle O_0(\boldsymbol{k}_1) O_0(\boldsymbol{k}_2) O_0(\boldsymbol{k}_3) \rangle'$$

$$= -2g_3 \int_z \boldsymbol{K_{k_1}}(z) \boldsymbol{K_{k_2}}(z) \boldsymbol{K_{k_3}}(z)$$

$$\qquad - 2a_2 \int_z \partial_M \boldsymbol{E}(z) \left[\partial^M \boldsymbol{K_{k_1}}(z) \partial_N \boldsymbol{K_{k_2}}(z) \partial^N \boldsymbol{K_{k_3}}(z) + (231) + (312) \right]$$

$$\qquad + (-2g_3)^2 \int_{z,z'} \left[\widetilde{\boldsymbol{E}}(z) \boldsymbol{K_{k_1}}(z) \boldsymbol{G_{k_1}}(z,z') \boldsymbol{K_{k_2}}(z') \boldsymbol{K_{k_3}}(z') + (231) + (312) \right]$$

$$\qquad + 2g_3 a_2 \int_{z,z'} \Big[\boldsymbol{K_{k_1}}(z) \boldsymbol{K_{k_2}}(z) \partial'_M \boldsymbol{G_{k_3}}(z,z')$$

$$\qquad\qquad\qquad \times \Big(\partial'^M \boldsymbol{K_{k_3}}(z') \partial'_N \boldsymbol{E}(z') \partial'^N \boldsymbol{E}(z') + 2 \partial'^M \boldsymbol{E}(z') \partial'_N \boldsymbol{E}(z') \partial'^N \boldsymbol{K_{k_3}}(z') \Big)$$

$$\qquad\qquad\qquad + (231) + (312) \Big] \tag{A.42}$$

$$= -2g_3 \int \frac{dz}{z^4} \boldsymbol{K_{k_1}}(z) \boldsymbol{K_{k_2}}(z) \boldsymbol{K_{k_3}}(z) \tag{A.43}$$

$$\qquad - 2a_2 \int dz \Big[3 \partial_z \boldsymbol{K_{k_1}}(z) \partial_z \boldsymbol{K_{k_2}}(z) \partial_z \boldsymbol{K_{k_3}}(z) \partial_z \boldsymbol{E}(z)$$

$$\qquad\qquad\qquad - \Big(\boldsymbol{k}_1.\boldsymbol{k}_2 \boldsymbol{K_{k_1}}(z) \boldsymbol{K_{k_2}}(z) \partial_z \boldsymbol{K_{k_3}}(z) \partial_z \boldsymbol{E}(z) + (231) + (312) \Big) \Big] \tag{A.44}$$

$$\qquad + \dots .$$

Here we dropped the other integrals because they turn out to be subleading in λ and so only the first and second integrals (A.43), (A.44) contribute to the three-point function. The first integral (A.43) comes from (A.30) while the second comes from the first integral of (A.32).

B Explicit form of the correlation functions at all orders

In this appendix, we evaluate the effective bulk-boundary propagators $\boldsymbol{E}$ and $\boldsymbol{K_q}$ explicitly at the leading order in λ. The non-derivative part of the three-point function will also be evaluated.

B.1 Zero-momentum bulk-boundary effective propagator

Let us compute $E_n^{(g_3)}(z)$ at the leading order in λ. We will encounter the following integral

$$\int_0^\infty \frac{dz'}{z'^4} z'^{a\lambda} z'^{b\lambda} \mathcal{G}_{\mathbf{0}}(z, z'), \tag{B.1}$$

where the zero-momentum bulk-bulk propagator reads

$$\mathcal{G}_{\mathbf{0}}(z, z') = \frac{1}{3 - 2\lambda} \left[z^\lambda z'^{3-\lambda} \theta(z - z') + z'^\lambda z^{3-\lambda} \theta(z' - z) \right]. \tag{B.2}$$

By the step functions in $\mathcal{G}_{\mathbf{0}}$, the integral splits into $\int_0^z$ and $\int_z^\infty$ parts. The $\int_z^\infty$ part has an integrand $z'^{(a+b+1)\lambda-4}$, so that the integral is convergent around $z \sim \infty$. Also it is regular at $\lambda = 0$. On the other hand, $\int_0^z$ part has integrand $z'^{-1+(a+b-1)\lambda}$ and the leading order of the integral is of $\mathcal{O}(\lambda^{-1})$. Thus the integral becomes

$$\int_0^\infty \frac{dz'}{z'^4} z'^{a\lambda} z'^{b\lambda} \mathcal{G}_0(z, z') = \frac{z^{(a+b)\lambda}}{3(a + b - 1)\lambda} + \dots, \tag{B.3}$$

where the dots stand for higher order terms in λ. Here one would wonder if we may approximate that $z^{(a+b)\lambda} \simeq 1$ at the leading order in λ. However, this approximation breaks down when $\lambda \ln|z| \gtrsim 1$ (indeed, it happens for very small z in the integral region $[0, \infty)$). We therefore keep $z^{(a+b)\lambda}$ without reducing it to 1. This remark applies to the computations in what follows. With the explicit forms for $n = 1$ and $n = 2$

$$E_1^{(g_3)}(z) = z^\lambda, \qquad E_2^{(g_3)}(z) = \frac{z^{2\lambda}}{6\lambda}, \tag{B.4}$$

the recursive definition of $E_n^{(g_3)}$ given by (A.23) and (A.24) yields

$$E_n^{(g_3)}(z) = \frac{z^{n\lambda}}{(6\lambda)^{n-1}}. \tag{B.5}$$

Order estimate of the integral (A.42) **for three-point function.** Using this explicit form (B.5), we can estimate the λ-order of the integral (A.42) for the three-point function to show that (A.43) and (A.44) dominate.[16] The point is that one z-differentiation of the effective zero-momentum propagator $E_{n+1}^{(g_3)}(z)$ yields one λ. By this property, we can see for each order in $\bar{\phi}$, or equivalently in g_3, that the 1st and 2nd term on the right hand side of (A.42) always dominate over the 3rd and 4th terms at the leading order in λ.

---

[16] The following order estimate can be justified recursively.

B.2 Effective bulk-boundary propagators of general momentum

Let us compute $K_{n,\boldsymbol{q}}(z)$. We start from $K_{1,\boldsymbol{q}}(z) = \mathcal{K}_{\boldsymbol{q}}(z)$. Applying the recursion relation (A.26) to this, we find

$$K_{2,\boldsymbol{q}}(z) = \int_0^\infty \frac{dz'}{z'^4} \mathcal{G}_{\boldsymbol{q}}(z,z') E_1^{(g_3)}(z') \mathcal{K}_{\boldsymbol{q}}(z'). \tag{B.6}$$

The bulk-to-boundary propagator may be expanded as

$$\mathcal{K}_{\boldsymbol{q}}(z) = q^{-\lambda} \left\{ (qz)^\lambda \left[1 + \mathcal{O}\left((qz)^2\right) \right] + \frac{1}{3}(qz)^{3-\lambda} \left[1 + \mathcal{O}\left((qz)^2\right) \right] \right\}. \tag{B.7}$$

Note that the series expansion is in the the dimensionless combination qz. Here and in what follows, we will recurrently use such a dimensionless combination. It will make the computations simpler and also be useful to reproduce the correct scale-dependence of the correlation functions.

The $z > z'$ part of the bulk-to-bulk propagator may be expanded as

$$\mathcal{G}_{\boldsymbol{q}}(z,z') = \mathcal{K}_{\boldsymbol{q}}(z) \mathcal{I}_{\boldsymbol{q}}(z') = q^{-3+\lambda} \mathcal{K}_{\boldsymbol{q}}(z) \frac{\Gamma(3/2-\lambda)}{2\Gamma(5/2-\lambda)} (qz')^{3-\lambda} \left[1 + \mathcal{O}\left((qz')^2\right) \right], \tag{B.8}$$

where we introduced

$$\mathcal{I}_{\boldsymbol{q}}(z) = 2^{1/2-\lambda} \Gamma(3/2-\lambda)(qz)^{3/2} q^{-3+\lambda} I_{3/2-\lambda}(qz). \tag{B.9}$$

For $\lambda \ll 1$, we may simplify it as

$$\mathcal{G}_{\boldsymbol{q}}(z,z') \simeq \frac{1}{3} q^{-3+\lambda} \mathcal{K}_{\boldsymbol{q}}(z)(qz')^{3-\lambda} \left[1 + \mathcal{O}\left((qz')^2\right) \right]. \tag{B.10}$$

Note that we ignored λ in the Gamma functions but kept $(qz')^{3-\lambda}$. This is because the approximation $(qz)^\lambda \simeq 1$ is not valid when $\lambda |\ln(qz)| \gtrsim 1$, as explained in the zero-momentum case. On the other hand, the $z' > z$ part may be expanded as

$$\mathcal{G}_{\boldsymbol{q}}(z,z') = q^{-\lambda} \mathcal{I}_{\boldsymbol{q}}(z) \left[(qz')^\lambda \left(1 + \mathcal{O}\left((qz')^2\right) \right) + \frac{1}{3}(qz')^{3-\lambda} \left(1 + \mathcal{O}\left((qz')^2\right) \right) \right]. \tag{B.11}$$

The recursion relation for $n = 2$ (B.6) reads, reflecting the step functions in $\mathcal{G}_{\boldsymbol{q}}$,

$$K_{2,\boldsymbol{q}}(z) = \left(\int_0^z + \int_z^\infty \right) \frac{dz'}{z'^4} \mathcal{G}_{\boldsymbol{q}}(z,z') E_1^{(g_3)}(z') \mathcal{K}_{\boldsymbol{q}}(z'). \tag{B.12}$$

The first part is

$$\int_0^z \text{part} \simeq q^{-\lambda} \mathcal{K}_{\boldsymbol{q}}(z) \int_0^{qz} \frac{dy'}{y'^4} \frac{1}{3} y'^{3+\lambda} \left[1 + \mathcal{O}\left(y'^2\right) \right], \quad y' = qz', \tag{B.13}$$

whose dominant contribution is from $y' \sim 0$. We can find the leading order terms in λ by collecting the $y'^{-1+\mathcal{O}(\lambda)}$ terms in the integrand. The remaining part of (B.12) is

$$\int_z^\infty \text{part} \simeq q^{3-3\lambda} \mathcal{I}_q(z) \left(\int_0^\infty - \int_0^{qz} \right) \frac{dy'}{y'^4} y'^\lambda \left[y'^\lambda \left(1 + \mathcal{O}\left(y'^2\right) \right) + \frac{1}{3} y'^{3-\lambda} \left(1 + \mathcal{O}\left(y'^2\right) \right) \right]^2. \tag{B.14}$$

Its dominant contribution is again from $y' \sim 0$ since the integrand is originally proportional to $y'^{\lambda-4}\mathcal{K}_{\boldsymbol{q}}^2(y')$, which damps exponentially as $y' \to \infty$. Therefore the leading order terms in λ can be found by collecting the $y'^{-1+\mathcal{O}(\lambda)}$ terms and applying (C.7) to them. Then it turns out that the contributions from $\int_0^\infty$ and $\int_0^{qz}$ differ by an overall factor of $(qz)^\lambda$, which is not negligible when $\lambda|\ln(qz)| \gtrsim 1$. Whether it is negligible is determined by whether the (qz)-integral to which the effective propagator is applied is regular around $qz = 0$ or not. We will discuss this point for the integrals (A.43) and (A.44), respectively.

B.2.1 Effective propagators in integral (A.43)

Let us consider the case in which the effective propagators are used in the integral (A.43). We first estimate the order in λ. For this, following the technique given in appendix C, we collect terms of the form $z^{-1+\mathcal{O}(\lambda)}$, which gives rise to λ^{-1}. Indeed the integral (A.43) contains $z^{-1+\mathcal{O}(\lambda)}$. So the λ-expansion of this integral starts from order λ^{-1}. Since this integrand $z^{-1+\mathcal{O}(\lambda)}$ is singular around $z = 0$, it is dangerous to set $(qz)^\lambda = 1$ and thus (B.14) cannot be zero.

To extract the leading order in λ from the integral (B.12), namely (B.13)+(B.14), we collect terms of the form $y'^{-1+\mathcal{O}(\lambda)}$ following appendix C. Then we find

$$K_{2,\boldsymbol{q}}(z) = q^{-2\lambda}\lambda^{-1}\left[\frac{2}{9}(qz)^{3-\lambda} - \frac{1}{9}(qz)^3 + \frac{1}{3}(qz)^{2\lambda} + \text{higher order in } \lambda\right]. \tag{B.15}$$

Using the recursion relation (A.27), we can find the structure of $K_{n+1,\boldsymbol{q}}(z)$ inductively

$$K_{n+1,\boldsymbol{q}}(z) = q^{-(n+1)\lambda}\lambda^{-n}\left[A_n(qz)^{(n+1)\lambda} + \sum_{l=0}^{n} B_{nl}(qz)^{3+(l-1)\lambda}\right], \tag{B.16}$$

where A_n, B_{nl} are independent of λ.

Let us evaluate the integral (A.43). This involves three momenta k_1, k_2, k_3. We introduce $k = k_1 + k_2 + k_3$ as a reference momentum and rescale the integration variable as $y = kz$. (See also appendix C.) We can then use the approximation $(k_i/k)^\lambda \sim 1$ by the approximation (4.5). Then, we can show at the leading order in λ that the integral is proportional to $k_1^{3-3\lambda} + k_2^{3-3\lambda} + k_3^{3-3\lambda}$ at all orders in $\bar{\phi}$. The proportional factor is the function of $\bar{\phi}k^{-\lambda}$, which is fixed in section 4.2.

B.2.2 Effective propagators in integral (A.44)

Let us next consider the case in which the effective propagators are used in the integral (A.44). We first estimate the order in λ. In this case it turns out that the leading contribution in the λ-expansion comes from the terms in the integrand which are regular around $z = 0$. So we may set $(qz)^\lambda = 1$ and thus (B.14) becomes zero. Thus it is enough to evaluate the $[0, z]$-part (B.13). Then, $K_{2,\boldsymbol{q}}(z)$ becomes

$$K_{2,\boldsymbol{q}}(z) = \frac{z^\lambda}{3\lambda}\mathcal{K}_{\boldsymbol{q}}(z). \tag{B.17}$$

For $K_{n,\boldsymbol{q}}(z)$ with general n, it is also enough to evaluate the z'-integral over $[0, z]$ in the recursion relation (A.27). We then find

$$K_{n+1,\boldsymbol{q}}(z) = (n+1)\left(\frac{z^\lambda}{6\lambda}\right)^n \mathcal{K}_{\boldsymbol{q}}(z). \tag{B.18}$$

Let us find explicit forms of $\boldsymbol{K}_{\boldsymbol{q}}(z)$ and $\boldsymbol{E}(z)$. Here $\boldsymbol{q}$ is one of the three-momenta $\boldsymbol{k}_1, \boldsymbol{k}_2, \boldsymbol{k}_3$ in the three-point function of our interest. Before taking the infinite sum in the definitions (A.34) and (A.35) of $\boldsymbol{E}$ and $\boldsymbol{K}_{\boldsymbol{q}}$, let us clarify the power structure of $\boldsymbol{K}_{\boldsymbol{q}}(z)$ and $\boldsymbol{E}(z)$. As in the non-derivative case, we rescale the integration variable with the reference momentum k as $y = kz$ in (A.43) and (A.44). Then we can see that $-\bar{\phi}^{-1}\boldsymbol{E}$ and $\boldsymbol{K}_{\boldsymbol{q}}$ are the power series in the following form: for each n

$$(-\bar{\phi})^n E_n^{(g_3)}, \quad (-\bar{\phi})^{n-1} K_{n,\boldsymbol{q}}^{(g_3)} \quad \propto \quad \left(\frac{-\bar{\phi}k^{-\lambda}}{\lambda}\right)^n (1 + \mathcal{O}(\lambda)),$$

where the approximation (4.5) was applied. Therefore, in the IR scale characterized by $\bar{\phi}k^{-\lambda}/\lambda = \mathcal{O}(1)$, it is enough to pick up the λ-leading contributions to $K_{n,\boldsymbol{q}}$ and $-\bar{\phi}^{-1}E_n^{(g_3)}$ for each n in order to extract the λ-leading contributions to (A.34) and (A.35). Substituting (B.5) and (B.18) into the definitions (A.34) and (A.35), we find

$$\boldsymbol{K}_{\boldsymbol{q}}(z) = \left(1 - \frac{g_3\bar{\phi}z^\lambda}{3\lambda}\right)^{-2} \mathcal{K}_{\boldsymbol{q}}(z), \tag{B.19}$$

$$\boldsymbol{E}(z) = (-\bar{\phi})\left(1 - \frac{g_3\bar{\phi}z^\lambda}{3\lambda}\right)^{-1} z^\lambda. \tag{B.20}$$

Since we can use the approximation $(kz)^\lambda = 1$ inside the integral (A.44), these forms can be simplified further,

$$\boldsymbol{K}_{\boldsymbol{q}}(z) = \left(1 - \frac{g_3\bar{\phi}k^{-\lambda}}{3\lambda}\right)^{-2} \mathcal{K}_{\boldsymbol{q}}(z), \tag{B.21}$$

$$\boldsymbol{E}(z) = (-\bar{\phi})\left(1 - \frac{g_3\bar{\phi}k^{-\lambda}}{3\lambda}\right)^{-1} z^\lambda. \tag{B.22}$$

Similarly, we may simplify $\boldsymbol{K}'_{\boldsymbol{k}_i}(z)$ and $\boldsymbol{E}'(z)$ as

$$\boldsymbol{K}'_{\boldsymbol{q}}(z) = \left(1 - \frac{g_3\bar{\phi}k^{-\lambda}}{3\lambda}\right)^{-2} \mathcal{K}'_{\boldsymbol{q}}(z), \tag{B.23}$$

$$\boldsymbol{E}'(z) = (-\lambda\bar{\phi})\left(1 - \frac{g_3\bar{\phi}k^{-\lambda}}{3\lambda}\right)^{-2} z^{\lambda-1}. \tag{B.24}$$

B.3 From AdS to dS

We have obtained from the AdS action (A.1) the integral expressions for the full two-point and three-point functions and the explicit forms of the effective propagators. Now, following section 3.3, we convert them into the forms associated with the UV CFT dual to our inflation model (in dS). To achieve this, we apply the replacement (3.20) after recovering the AdS radius dependence using the rule (A.19). The result is the following:

(i) Effective bulk-boundary propagators for (A.44)

$$\boldsymbol{K}_{\boldsymbol{q}}^{\mathrm{dS}}(z) = \left(1 + \frac{g_3 R_{\mathrm{dS}}^{-2}\bar{\phi}k^{-\lambda}}{3\lambda}\right)^{-2}\mathcal{K}_{\boldsymbol{q}}(z),\tag{B.25}$$

$$\boldsymbol{E}^{\mathrm{dS}}(z) = -\bar{\phi}\left(1 + \frac{g_3 R_{\mathrm{dS}}^{-2}\bar{\phi}k^{-\lambda}}{3\lambda}\right)^{-1}z^{\lambda}.\tag{B.26}$$

Their derivatives corresponding to (B.23) and (B.24) may also be obtained in a similar way.

(ii) Integral form of the two-point function

$$\langle O_0(\boldsymbol{q})O_0(-\boldsymbol{q})\rangle' = -R_{\mathrm{dS}}^2\boldsymbol{K}_{\boldsymbol{q}}(z)\big|_{[3-2\lambda]} + \sum_{m\geq 2}\frac{2m}{2^m}\alpha_m(R_{\mathrm{dS}})^{2(m-2)}\times$$
$$\times \int_0^\infty dz\,z^{2(m-2)}\boldsymbol{E}'(z)^{2(m-1)}\left\{(2m-1)\boldsymbol{K}_{\boldsymbol{q}}'(z)^2 - \boldsymbol{q}^2\boldsymbol{K}_{\boldsymbol{q}}(z)^2\right\}.\tag{B.27}$$

(iii) Integral form of the three-point function

$$\langle O_0(\boldsymbol{k}_1)O_0(\boldsymbol{k}_2)O_0(\boldsymbol{k}_3)\rangle'$$
$$= -2g_3\int_z \boldsymbol{K}_{\boldsymbol{k}_1}(z)\boldsymbol{K}_{\boldsymbol{k}_2}(z)\boldsymbol{K}_{\boldsymbol{k}_3}(z) + \sum_{m\geq 2}\frac{m(m-1)}{2^{m-2}}\alpha_m(R_{\mathrm{dS}})^{2(m-2)}\times$$
$$\times \int_0^\infty dz\,z^{2(m-2)}\boldsymbol{E}'(z)^{2m-3}\Big\{(2m-1)\boldsymbol{K}_{\boldsymbol{k}_1}'(z)\boldsymbol{K}_{\boldsymbol{k}_2}'(z)\boldsymbol{K}_{\boldsymbol{k}_3}'(z)$$
$$- \Big(\boldsymbol{k}_1.\boldsymbol{k}_2\boldsymbol{K}_{\boldsymbol{k}_1}(z)\boldsymbol{K}_{\boldsymbol{k}_2}(z)\boldsymbol{K}_{\boldsymbol{k}_3}'(z) + (231) + (312)\Big)\Big\}.\tag{B.28}$$

C three-point functions with two nearly marginal scalars

In this appendix we compute CFT three-point functions

$$\langle O_1(\boldsymbol{k}_1)O_2(\boldsymbol{k}_2)O_3(\boldsymbol{k}_3)\rangle'_{\mathrm{CFT}}\tag{C.1}$$

of two nearly marginal scalars, O_1 and O_2, and one scalar O_3 with a conformal dimension close to a non-negative integer n. More explicitly, we parametrize the dimension Δ_i of O_i as

$$\Delta_1 = 3 + v_1\lambda,\quad \Delta_2 = 3 + v_2\lambda,\quad \Delta_3 = n + v_3\lambda,\tag{C.2}$$

where $\lambda \ll 1$ characterizes the deviation from marginality and integer dimension, and we focus on the leading order in λ of the three-point functions.

As we mentioned earlier, a CFT three-point function of primary scalars of dimensions Δ_i ($i = 1, 2, 3$) can be uniquely fixed by the conformal symmetry as [50]

$$\langle O_1(\boldsymbol{k}_1)O_2(\boldsymbol{k}_2)O_3(\boldsymbol{k}_3)\rangle' = C_{123}k^{\Delta_1+\Delta_2+\Delta_3-3}I_{\frac{d}{2}-1\{\Delta_1-\frac{3}{2},\Delta_2-\frac{3}{2},\Delta_3-\frac{3}{2}\}}(\kappa_1,\kappa_2,\kappa_3)\tag{C.3}$$

up to the OPE coefficient C_{123}. Here we introduced $k = k_1 + k_2 + k_3$ and $\kappa_i = k_i/k$. We refer to the function $I_{\alpha\{\beta_1,\beta_2,\beta_3\}}$ as the triple-K integral [49–51] defined by[17]

$$I_{\alpha\{\beta_1,\beta_2,\beta_3\}}(\kappa_1, \kappa_2, \kappa_3) = \kappa_1^{\beta_1} \kappa_2^{\beta_2} \kappa_3^{\beta_3} \int_0^\infty dx\, x^\alpha K_{\beta_1}(\kappa_1 x) K_{\beta_2}(\kappa_2 x) K_{\beta_3}(\kappa_3 x)\,, \qquad (\text{C.4})$$

where $K_\nu(z)$ is the modified Bessel function of the second kind. Refs. [50, 51] studied properties of the triple-K integral in detail. Here we give a brief summary of their results we will use. The integral (C.4) converges if the parameters satisfy $\alpha + 1 > |\beta_1| + |\beta_2| + |\beta_3|$ for fixed $\kappa_1, \kappa_2, \kappa_3 > 0$. Outside this parameter region, we define the integral as its maximal analytical continuation such that the integral coincides with the integral evaluated in the convergence region. This integral, however, still has singularities for special parameter sets, defined by $\alpha + 1 \pm \beta_1 \pm \beta_2 \pm \beta_3 = -2n$ for $n = 0, 1, \ldots$, where the choice of the three $\pm$ is arbitrary. In particular, for our parameter set (C.2), the triple-K integral is singular in the limit $\lambda \to 0$. In the following we compute the triple-K integral for (C.2) at the leading order in λ by applying the discussion in [51].

C.1 General results

By using the series expansion of the Bessel K function,

$$K_\nu(z) = \sum_{j=0}^\infty \left[a_j^-(\nu) z^{-\nu+2j} + a_j^+(\nu) z^{\nu+2j} \right] \quad \text{with} \quad a_j^\pm(\nu) := \frac{(-)^j \Gamma(\mp\nu - j)}{2^{\pm\nu+2j+1} j!}\,, \qquad (\text{C.5})$$

we notice that the integrand of the triple-K integral of our interest contains terms schematically of the form,

$$\sim \sum_{j=0}^\infty x^{-1\pm n+2j+\mathcal{O}(\lambda)}\,, \quad \sum_{j=0}^\infty x^{-1\pm(n-3)+2j+\mathcal{O}(\lambda)}\,, \quad \sum_{j=0}^\infty x^{-1-(n-6)+2j+\mathcal{O}(\lambda)}\,. \qquad (\text{C.6})$$

Here for notational simplicity we omitted the coefficients of each term, which are of $\mathcal{O}(\lambda^0)$. An important point is that there always appear $x^{-1+\mathcal{O}(\lambda)}$-terms when $n \geq 0$, i.e., when O_3 has a non-negative dimension close to an integer. Since $\int dx\, x^{-1+\alpha\lambda} = \frac{1}{\alpha\lambda} x^{\alpha\lambda}$, one may naively expect that the singularity of the triple-K integral in the $\lambda \to 0$ limit is associated with those $x^{-1+\mathcal{O}(\lambda)}$-terms. Indeed, ref. [51] showed that the singularity in this limit arises only from the integration over a region around $x = 0$ of $x^{-1+\mathcal{O}(\lambda)}$-terms, by virtue of the maximal analytic continuation. Based on the argument in [51], we apply the following recipe to compute the triple-K integral at the leading order in λ:

1. Expand the integrand of the triple-K integral (C.4) in x using (C.5).

2. Then, collect the $x^{-1+\mathcal{O}(\lambda)}$-terms and integrate them over a region around $x = 0$ using

$$\int_0^\mu dx\, x^{-1+\alpha\lambda} = \frac{1}{\alpha\lambda} \mu^{\alpha\lambda} = \frac{1}{\alpha\lambda} \left[1 + \mathcal{O}(\alpha\lambda \ln \mu) \right]\,, \qquad (\text{C.7})$$

where $\mu \ll 1$ is the cutoff satisfying the condition $|\alpha\lambda \ln \mu| \ll 1$.

---

[17]Note that the triple-K integrals take the same form, up to an overall numerical constant, as the three-point correlation function computed with the Witten diagrams in $(d+1)$-dimensional AdS spacetime, in which the coefficient C_{123} is determined from the bulk action in AdS_{d+1}, and the x-integral in (C.4) corresponds to the integral in the radial direction of AdS_{d+1}.

This procedure gives us the leading contribution to the triple-K integrals in the λ expansion.

Now it is straightforward to compute the triple-K integral. Below, we first explain the computation for the $n = 0$ case in detail, and then present the results for general n.

Detailed explanation for n = 0. We start from a detailed explanation for the $n = 0$ case. In this case, the integrand has three types of $x^{-1+\mathcal{O}(\lambda)}$-terms:

$$
x^{-1-(v_1+v_2+v_3)\lambda} a_0^- \left(\frac{3}{2} + v_1\lambda \right) a_0^- \left(\frac{3}{2} + v_2\lambda \right) a_0^- \left(-\frac{3}{2} + v_3\lambda \right)
$$
$$
+ (\kappa_1)^{3+2v_1\lambda}(\kappa_3)^{-3+2v_3\lambda} x^{-1+(v_1-v_2+v_3)\lambda} a_0^+ \left(\frac{3}{2} + v_1\lambda \right) a_0^- \left(\frac{3}{2} + v_2\lambda \right) a_0^+ \left(-\frac{3}{2} + v_3\lambda \right)
$$
$$
+ (\kappa_2)^{3+2v_2\lambda}(\kappa_3)^{-3+2v_3\lambda} x^{-1+(-v_1+v_2+v_3)\lambda} a_0^- \left(\frac{3}{2} + v_1\lambda \right) a_0^+ \left(\frac{3}{2} + v_2\lambda \right) a_0^+ \left(-\frac{3}{2} + v_3\lambda \right).
$$
$$(C.8)$$

By applying eq. (C.7), we find

$$
I_{\frac{1}{2}\{\frac{3}{2}+v_1\lambda,\frac{3}{2}+v_2\lambda,-\frac{3}{2}+v_3\lambda\}}(k_1, k_2, k_3)
$$
$$
= \frac{a_0^- (\frac{3}{2}) a_0^- (\frac{3}{2}) a_0^- (-\frac{3}{2})}{-(v_1 + v_2 + v_3)\lambda} + \left(\frac{\kappa_1}{\kappa_3} \right)^3 \frac{a_0^+ (\frac{3}{2}) a_0^- (\frac{3}{2}) a_0^+ (-\frac{3}{2})}{(v_1 - v_2 + v_3)\lambda}
$$
$$
+ \left(\frac{\kappa_2}{\kappa_3} \right)^3 \frac{a_0^- (\frac{3}{2}) a_0^+ (\frac{3}{2}) a_0^+ (-\frac{3}{2})}{(-v_1 + v_2 + v_3)\lambda} + \mathcal{O}(\lambda^0)
$$
$$
= \frac{\pi^{3/2}}{6\sqrt{2}\,\lambda} \left[\frac{1}{-(v_1 + v_2 + v_3)} + \frac{(\kappa_1/\kappa_3)^3}{v_1 - v_2 + v_3} + \frac{(\kappa_2/\kappa_3)^3}{-v_1 + v_2 + v_3} \right] + \mathcal{O}(\lambda^0). \quad (C.9)
$$

Here we have used $(\kappa_i)^\lambda = 1 + \lambda \ln \kappa_i + \ldots = 1 + \mathcal{O}(\lambda)$. This approximation is applicable as long as $|\lambda \ln(k_i/k_t)| \ll 1$, which is indeed the case (4.5) in our inflationary discussions.

Three-point functions for n = 1, 2, 3. In a similar manner we may compute the integral for $n = 1, 2, 3$ as follows: for $n = 1$,

$$
I_{\frac{1}{2}\{\frac{3}{2}+v_1\lambda,\frac{3}{2}+v_2\lambda,-\frac{1}{2}+v_3\lambda\}}(\kappa_1, \kappa_2, \kappa_3) = \frac{\pi^{3/2}}{4\sqrt{2}(v_1 + v_2 - v_3)\lambda} \frac{(\kappa_1)^2 + (\kappa_2)^2 - (\kappa_3)^2}{\kappa_3} + \mathcal{O}(\lambda^0). \quad (C.10)
$$

For $n = 2$,

$$
I_{\frac{1}{2}\{\frac{3}{2}+v_1\lambda,\frac{3}{2}+v_2\lambda,\frac{1}{2}+v_3\lambda\}}(\kappa_1, \kappa_2, \kappa_3) = \frac{\pi^{3/2}}{4\sqrt{2}(v_1 + v_2 + v_3)\lambda} \left[(\kappa_1)^2 + (\kappa_2)^2 - (\kappa_3)^2 \right] + \mathcal{O}(\lambda^0). \quad (C.11)
$$

For $n = 3$,

$$
I_{\frac{1}{2}\{\frac{3}{2}+v_1\lambda,\frac{3}{2}+v_2\lambda,\frac{3}{2}+v_3\lambda\}}(\kappa_1, \kappa_2, \kappa_3)
$$
$$
= \frac{\pi^{3/2}}{6\sqrt{2}\lambda} \left[\frac{(\kappa_3)^3}{-v_1 - v_2 + v_3} + \frac{(\kappa_2)^3}{-v_1 + v_2 - v_3} + \frac{(\kappa_1)^3}{v_1 - v_2 - v_3} \right] + O(\lambda^0). \quad (C.12)
$$

In particular, when $v_1 = v_2 = v_3 = -1$, i.e., $\Delta_1 = \Delta_2 = \Delta_3 = 3 - \lambda$, it reduces to the form,

$$
I_{\frac{1}{2}\{\frac{3}{2}-\lambda,\frac{3}{2}-\lambda,\frac{3}{2}-\lambda\}}(\kappa_1, \kappa_2, \kappa_3) = \frac{\pi^{3/2}}{6\sqrt{2}\lambda} \left[(\kappa_1)^3 + (\kappa_2)^3 + (\kappa_3)^3 \right] + O(\lambda^0). \quad (C.13)
$$

General expression for $n \geq 4$. It is not difficult to derive the general expression for $n \geq 4$. For an even $n \geq 4$, we have

$$
\begin{aligned}
I_{\frac{1}{2}\{\frac{3}{2}+v_1\lambda, \frac{3}{2}+v_2\lambda, n-\frac{3}{2}+v_3\lambda\}}(\kappa_1, \kappa_2, \kappa_3) \\
= -\frac{(-)^{\frac{n}{2}}}{2^{\frac{3}{2}}(v_1+v_2+v_3)\lambda} \times \\
\times \sum_{\substack{j_1+j_2+j_3=\frac{n}{2} \\ j_1, j_2, j_3 \geq 0}} \frac{(\kappa_1)^{2j_1}(\kappa_2)^{2j_2}(\kappa_3)^{2j_3}}{j_1! j_2! j_3!} \Gamma\left(\frac{3}{2}-j_1\right)\Gamma\left(\frac{3}{2}-j_2\right)\Gamma\left(n-\frac{3}{2}-j_3\right) \\
- \frac{(-)^{\frac{n}{2}}(\kappa_1)^3(\kappa_2)^3}{2^{\frac{3}{2}}(v_1+v_2-v_3)\lambda} \times \\
\times \sum_{\substack{j_1+j_2+j_3=\frac{n-6}{2} \\ j_1, j_2, j_3 \geq 0}} \frac{(\kappa_1)^{2j_1}(\kappa_2)^{2j_2}(\kappa_3)^{2j_3}}{j_1! j_2! j_3!} \Gamma\left(-\frac{3}{2}-j_1\right)\Gamma\left(-\frac{3}{2}-j_2\right)\Gamma\left(n-\frac{3}{2}-j_3\right) \\
+ O(\lambda^0),
\end{aligned}
\tag{C.14}
$$

where the second term should be omitted when $n = 4$. Similarly, a general expression for an odd $n \geq 5$ is

$$
\begin{aligned}
I_{\frac{1}{2}+u\lambda\{\frac{3}{2}+v_1\lambda, \frac{3}{2}+v_2\lambda, n-\frac{3}{2}+v_3\lambda\}}(\kappa_1, \kappa_2, \kappa_3) \\
= \frac{(-)^{\frac{n+3}{2}}(\kappa_2)^3}{2^{\frac{3}{2}}(-v_1+v_2-v_3)\lambda} \times \\
\times \sum_{\substack{j_1+j_2+j_3=\frac{n-3}{2} \\ j_1, j_2, j_3 \geq 0}} \frac{(\kappa_1)^{2j_1}(\kappa_2)^{2j_2}(\kappa_3)^{2j_3}}{j_1! j_2! j_3!} \Gamma\left(\frac{3}{2}-j_1\right)\Gamma\left(-\frac{3}{2}-j_2\right)\Gamma\left(n-\frac{3}{2}-j_3\right) \\
+ \frac{(-)^{\frac{n+3}{2}}(\kappa_1)^3}{2^{\frac{3}{2}}(v_1-v_2-v_3)\lambda} \times \\
\times \sum_{\substack{j_1+j_2+j_3=\frac{n-3}{2} \\ j_1, j_2, j_3 \geq 0}} \frac{(\kappa_1)^{2j_1}(\kappa_2)^{2j_2}(\kappa_3)^{2j_3}}{j_1! j_2! j_3!} \Gamma\left(-\frac{3}{2}-j_1\right)\Gamma\left(\frac{3}{2}-j_2\right)\Gamma\left(n-\frac{3}{2}-j_3\right) \\
+ O(\lambda^0).
\end{aligned}
\tag{C.15}
$$

C.2 Squeezed limit

We then discuss the squeezed limit $\kappa_1 \ll \kappa_2 = \kappa_3 = \kappa$ of the triple-K integral obtained in the previous subsection. For $n = 0, 1, 2, 3$, we may use the concrete expressions (C.9)–(C.12) to conclude that the triple-K integral for $n = 1, 2$ vanishes in the squeezed limit for arbitrary v_i's, whereas that for $n = 0, 3$, it does not vanish for a generic set of v_i's. For an

even $n \geq 4$, the squeezed limit is

$$
\lim_{\kappa_1 \to 0} I_{\frac{1}{2}\{\frac{3}{2}+v_1\lambda, \frac{3}{2}+v_2\lambda, n-\frac{3}{2}+v_3\lambda\}}(\kappa_1, \kappa, \kappa)
$$
$$
= -\frac{(-)^{\frac{n}{2}} \Gamma\left(\frac{3}{2}\right) \kappa^n}{2^{\frac{3}{2}}(v_1 + v_2 + v_3)\lambda} \sum_{\substack{j_2+j_3=\frac{n}{2} \\ j_2, j_3 \geq 0}} \frac{\Gamma\left(\frac{3}{2} - j_2\right) \Gamma\left(n - \frac{3}{2} - j_3\right)}{j_2! j_3!} + O(\lambda^0). \qquad \text{(C.16)}
$$

Similarly, for an odd $n \geq 5$, we have

$$
\lim_{\kappa_1 \to 0} I_{\frac{1}{2}+u\lambda\{\frac{3}{2}+v_1\lambda, \frac{3}{2}+v_2\lambda, n-\frac{3}{2}+v_3\lambda\}}(\kappa_1, \kappa, \kappa)
$$
$$
= \frac{(-)^{\frac{n+3}{2}} \Gamma\left(\frac{3}{2}\right) \kappa^n}{2^{\frac{3}{2}}(-v_1 + v_2 - v_3)\lambda} \sum_{\substack{j_2+j_3=\frac{n-3}{2} \\ j_2, j_3 \geq 0}} \frac{\Gamma\left(-\frac{3}{2} - j_2\right) \Gamma\left(n - \frac{3}{2} - j_3\right)}{j_2! j_3!} + O(\lambda^0). \qquad \text{(C.17)}
$$

Interestingly, by using the relation

$$
\sum_{j=0}^{m} \frac{\Gamma(-\alpha - j)\Gamma(m + \alpha + j)}{\Gamma(j+1)\Gamma(m-j+1)} = -\frac{\pi}{\alpha \sin \pi\alpha} \delta_{m,0}, \qquad \text{(C.18)}
$$

it turns out that eqs. (C.16) and (C.17) are identically zero. Note that it is easy to see that the first nonzero contribution in the squeezed limit is $\mathcal{O}((\kappa_1/\kappa)^2)$. We therefore conclude that the triple-K integrals associated with CFT three-point functions of two nearly marginal scalars and one scalar with the conformal dimension close to a non-negative integer n vanish in the squeezed limit, except for the case $n = 0, 3$, at the leading order in λ.

References

[1] J.M. Maldacena, *The Large-N limit of superconformal field theories and supergravity*, *Int. J. Theor. Phys.* **38** (1999) 1113 [*Adv. Theor. Math. Phys.* **2** (1998) 231] [`hep-th/9711200`] [INSPIRE].

[2] A. Strominger, *The dS/CFT correspondence*, *JHEP* **10** (2001) 034 [`hep-th/0106113`] [INSPIRE].

[3] E. Witten, *Quantum gravity in de Sitter space*, `hep-th/0106109` [INSPIRE].

[4] A. Strominger, *Inflation and the dS/CFT correspondence*, *JHEP* **11** (2001) 049 [`hep-th/0110087`] [INSPIRE].

[5] F. Larsen, J.P. van der Schaar and R.G. Leigh, *De Sitter holography and the cosmic microwave background*, *JHEP* **04** (2002) 047 [`hep-th/0202127`] [INSPIRE].

[6] J.M. Maldacena, *Non-Gaussian features of primordial fluctuations in single field inflationary models*, *JHEP* **05** (2003) 013 [`astro-ph/0210603`] [INSPIRE].

[7] F. Larsen and R. McNees, *Inflation and de Sitter holography*, *JHEP* **07** (2003) 051 [hep-th/0307026] [ɪɴSPIRE].

[8] J.P. van der Schaar, *Inflationary perturbations from deformed CFT*, *JHEP* **01** (2004) 070 [hep-th/0307271] [ɪɴSPIRE].

[9] D. Seery and J.E. Lidsey, *Non-gaussian inflationary perturbations from the dS/CFT correspondence*, *JCAP* **06** (2006) 001 [astro-ph/0604209] [ɪɴSPIRE].

[10] P. McFadden and K. Skenderis, *Holography for cosmology*, *Phys. Rev.* **D 81** (2010) 021301 [arXiv:0907.5542] [ɪɴSPIRE].

[11] P. McFadden and K. Skenderis, *The holographic universe*, *J. Phys. Conf. Ser.* **222** (2010) 012007 [arXiv:1001.2007] [ɪɴSPIRE].

[12] D. Anninos, T. Hartman and A. Strominger, *Higher spin realization of the dS/CFT correspondence*, arXiv:1108.5735 [ɪɴSPIRE].

[13] P. McFadden and K. Skenderis, *Holographic non-gaussianity*, *JCAP* **05** (2011) 013 [arXiv:1011.0452] [ɪɴSPIRE].

[14] A. Bzowski, P. McFadden and K. Skenderis, *Holographic predictions for cosmological 3-point functions*, *JHEP* **03** (2012) 091 [arXiv:1112.1967] [ɪɴSPIRE].

[15] M. Smolkin and N. Turok, *Dual description of a 4D cosmology*, arXiv:1211.1322 [ɪɴSPIRE].

[16] K. Schalm, G. Shiu and T. van der Aalst, *Consistency condition for inflation from (broken) conformal symmetry*, *JCAP* **03** (2013) 005 [arXiv:1211.2157] [ɪɴSPIRE].

[17] A. Bzowski, P. McFadden and K. Skenderis, *Holography for inflation using conformal perturbation theory*, *JHEP* **04** (2013) 047 [arXiv:1211.4550] [ɪɴSPIRE].

[18] I. Mata, S. Raju and S. Trivedi, *CMB from CFT*, *JHEP* **07** (2013) 015 [arXiv:1211.5482] [ɪɴSPIRE].

[19] J. Garriga and Y. Urakawa, *Inflation and deformation of conformal field theory*, *JCAP* **07** (2013) 033 [arXiv:1303.5997] [ɪɴSPIRE].

[20] D. Anninos, F. Denef, G. Konstantinidis and E. Shaghoulian, *Higher spin de Sitter holography from functional determinants*, *JHEP* **02** (2014) 007 [arXiv:1305.6321] [ɪɴSPIRE].

[21] P. McFadden, *On the power spectrum of inflationary cosmologies dual to a deformed CFT*, *JHEP* **10** (2013) 071 [arXiv:1308.0331] [ɪɴSPIRE].

[22] G.L. Pimentel, *Inflationary consistency conditions from a wavefunctional perspective*, *JHEP* **02** (2014) 124 [arXiv:1309.1793] [ɪɴSPIRE].

[23] A. Ghosh, N. Kundu, S. Raju and S.P. Trivedi, *Conformal invariance and the four point scalar correlator in slow-roll inflation*, *JHEP* **07** (2014) 011 [arXiv:1401.1426] [ɪɴSPIRE].

[24] J. Garriga and Y. Urakawa, *Holographic inflation and the conservation of ζ*, *JHEP* **06** (2014) 086 [arXiv:1403.5497] [ɪɴSPIRE].

[25] J. Garriga, K. Skenderis and Y. Urakawa, *Multi-field inflation from holography*, *JCAP* **01** (2015) 028 [arXiv:1410.3290] [ɪɴSPIRE].

[26] P. McFadden, *Soft limits in holographic cosmology*, *JHEP* **02** (2015) 053 [arXiv:1412.1874] [ɪɴSPIRE].

[27] N. Kundu, A. Shukla and S.P. Trivedi, *Ward identities for scale and special conformal transformations in inflation*, *JHEP* **01** (2016) 046 [arXiv:1507.06017] [ɪɴSPIRE].

[28] X. Chen, M.-x. Huang, S. Kachru and G. Shiu, *Observational signatures and non-Gaussianities of general single field inflation*, *JCAP* **01** (2007) 002 [hep-th/0605045] [iNSPIRE].

[29] V. Acquaviva, N. Bartolo, S. Matarrese and A. Riotto, *Second order cosmological perturbations from inflation*, *Nucl. Phys.* **B 667** (2003) 119 [astro-ph/0209156] [iNSPIRE].

[30] C. Armendariz-Picon, T. Damour and V.F. Mukhanov, *k-inflation*, *Phys. Lett.* **B 458** (1999) 209 [hep-th/9904075] [iNSPIRE].

[31] M. Alishahiha, E. Silverstein and D. Tong, *DBI in the sky*, *Phys. Rev.* **D 70** (2004) 123505 [hep-th/0404084] [iNSPIRE].

[32] D. Seery and J.E. Lidsey, *Primordial non-Gaussianities in single field inflation*, *JCAP* **06** (2005) 003 [astro-ph/0503692] [iNSPIRE].

[33] PLANCK collaboration, P.A.R. Ade et al., *Planck 2015 results. XIII. Cosmological parameters*, *Astron. Astrophys.* **594** (2016) A13 [arXiv:1502.01589] [iNSPIRE].

[34] H. Osborn, *Derivation of a four-dimensional c theorem*, *Phys. Lett.* **B 222** (1989) 97 [iNSPIRE].

[35] F. Baume, B. Keren-Zur, R. Rattazzi and L. Vitale, *The local Callan-Symanzik equation: structure and applications*, *JHEP* **08** (2014) 152 [arXiv:1401.5983] [iNSPIRE].

[36] P. Creminelli and M. Zaldarriaga, *Single field consistency relation for the 3-point function*, *JCAP* **10** (2004) 006 [astro-ph/0407059] [iNSPIRE].

[37] P. Creminelli, J. Noreña and M. Simonović, *Conformal consistency relations for single-field inflation*, *JCAP* **07** (2012) 052 [arXiv:1203.4595] [iNSPIRE].

[38] K. Hinterbichler, L. Hui and J. Khoury, *An infinite set of ward identities for adiabatic modes in cosmology*, *JCAP* **01** (2014) 039 [arXiv:1304.5527] [iNSPIRE].

[39] L. Berezhiani and J. Khoury, *Slavnov-Taylor identities for primordial perturbations*, *JCAP* **02** (2014) 003 [arXiv:1309.4461] [iNSPIRE].

[40] S.S. Gubser, I.R. Klebanov and A.M. Polyakov, *Gauge theory correlators from noncritical string theory*, *Phys. Lett.* **B 428** (1998) 105 [hep-th/9802109] [iNSPIRE].

[41] E. Witten, *Anti-de Sitter space and holography*, *Adv. Theor. Math. Phys.* **2** (1998) 253 [hep-th/9802150] [iNSPIRE].

[42] X. Chen and Y. Wang, *Quasi-single field inflation and non-gaussianities*, *JCAP* **04** (2010) 027 [arXiv:0911.3380] [iNSPIRE].

[43] D. Baumann and D. Green, *Signatures of supersymmetry from the early universe*, *Phys. Rev.* **D 85** (2012) 103520 [arXiv:1109.0292] [iNSPIRE].

[44] T. Noumi, M. Yamaguchi and D. Yokoyama, *Effective field theory approach to quasi-single field inflation and effects of heavy fields*, *JHEP* **06** (2013) 051 [arXiv:1211.1624] [iNSPIRE].

[45] N. Arkani-Hamed and J. Maldacena, *Cosmological collider physics*, arXiv:1503.08043 [iNSPIRE].

[46] F. Gliozzi, *More constraining conformal bootstrap*, *Phys. Rev. Lett.* **111** (2013) 161602 [arXiv:1307.3111] [iNSPIRE].

[47] F. Gliozzi and A. Rago, *Critical exponents of the 3D Ising and related models from conformal bootstrap*, *JHEP* **10** (2014) 042 [arXiv:1403.6003] [iNSPIRE].

[48] S. de Haro, S.N. Solodukhin and K. Skenderis, *Holographic reconstruction of space-time and renormalization in the AdS/CFT correspondence*, *Commun. Math. Phys.* **217** (2001) 595 [hep-th/0002230] [INSPIRE].

[49] A. Bzowski, P. McFadden and K. Skenderis, *Implications of conformal invariance in momentum space*, *JHEP* **03** (2014) 111 [arXiv:1304.7760] [INSPIRE].

[50] A. Bzowski, P. McFadden and K. Skenderis, *Scalar 3-point functions in CFT: renormalisation, β-functions and anomalies*, *JHEP* **03** (2016) 066 [arXiv:1510.08442] [INSPIRE].

[51] A. Bzowski, P. McFadden and K. Skenderis, *Evaluation of conformal integrals*, *JHEP* **02** (2016) 068 [arXiv:1511.02357] [INSPIRE].